RADIATION FROM A SHORT ELECTRIC DIPOLE ANTENNA IN A HOT UNIAXIAL PLASMA

Thesis by

Nagendra Singh

In Partial Fulfillment of the Requirements

For the Degree of

Doctor of Philosophy

California Institute of Technology

Pasadena, California

1971

(Submitted July 2, 1970)

ACKNOWLEDGMENTS

The author wishes to express his deep appreciation to his advisor, Professor Roy W. Gould, for his continued guidance, encouragement and constant interest throughout the course of this research.

The author is also indebted to Dr. Ray K. Fisher for his work on some of the experimental aspects of this problem. Thanks are extended to my colleagues, Mr. Vijay H. Arakeri and Mr. K. Palaniswami for their many helpful discussions and suggestions. Special thanks are extended to Mrs. Ruth Stratton, Mrs. Karen Current and Miss Carol Teeter for their excellent typing of the manuscript.

The author gratefully acknowledges the generous financial support he received from the California Institute of Technology. This work was supported in part by the U. S. Office of Naval Research and in part by the U. S. Atomic Energy Commission.

This work is dedicated to my brothers, Shri Raj Narain Singh and Shri Hridai Narain Singh.

ABSTRACT

The effects of electron temperature on the radiation fields and the resistance of a short dipole antenna embedded in a uniaxial plasma have been studied. It is found that for $\omega < \omega_p$ the antenna excites two waves, a slow wave and a fast wave. These waves propagate only within a cone whose axis is parallel to the biasing magnetostatic field $\underline{B}_o$ and whose semicone angle is slightly less than $\sin^{-1}(\omega/\omega_p)$. In the case of $\omega > \omega_p$ the antenna excites two separate modes of radiation. One of the modes is the electromagnetic mode, while the other mode is of hot plasma origin. A characteristic interference structure is noted in the angular distribution of the field. The far fields are evaluated by asymptotic methods, while the near fields are calculated numerically. The effects of antenna length ℓ, electron thermal speed, collisional and Landau damping on the near field patterns have been studied.

The input and the radiation resistances are calculated and are shown to remain finite for nonzero electron thermal velocities. The effect of Landau damping and the antenna length on the input and radiation resistances has been considered.

The radiation condition for solving Maxwell's equations is discussed and the phase and group velocities for propagation given. It is found that for $\omega < \omega_p$ in the radial direction (cylindrical coordinates) the power flow is in the opposite direction to that of the phase propagation. For $\omega > \omega_p$ the hot plasma mode has similar characteristics.

TABLE OF CONTENTS

I. INTRODUCTION

The behavior of an antenna in a magnetoplasma is of great interest from the viewpoints of ionospheric investigations and laboratory plasma diagnostics. The basic problem is to determine the impedance and the radiation field of the antenna. A major difficulty in predicting the behavior of an antenna in a plasma is the determination of valid boundary conditions. Other difficulties include the determination of current distribution on the source and the specifications of electromagnetic properties of the plasma. The sheath, surrounding the antenna, makes the accurate formulation of the boundary conditions and the analysis of the antenna properties a formidable task.

A number of investigators have studied this problem under various simplifying approximations. Some of the principal investigators are Bunkin [1], Kogelnik [2], Kuehl [3], Staras [4], Seshadri [5], Lee and Papas [6]. These authors have assumed a cold plasma model and have studied radiation from a given current distribution. Kogelnik [2] was the first to investigate the radiation resistance of an elementary dipole in a magneto-ionic medium. His formulation yields infinite radiation resistance for a point dipole for certain operating frequencies even though there is no loss mechanism present. Bunkin [1] and Kuehl [3] found far fields using the saddle point method. Their work shows that fields are infinite, for certain frequencies, on a conical surface (fig. 1.1) whose axis is along the magnetostatic field $\underline{B}_o$ and whose cone angle is determined by the plasma, the cyclotron and the operating frequencies. For a uniaxial plasma ($\underline{B}_o = \infty$) the half-cone angle is

given by $\sin^{-1}(\omega/\omega_p)$ where ω and ω_p are the operating and the plasma frequencies, respectively. The radiation is confined within the cone; there is no radiation outside the cone. The nature of infinity in the fields is such that the power flow from the antenna carrying a finite current is infinite. This manifestation of infinity in the fields and power radiated is well known in the literature by the name "infinity catastrophe". These results are unrealistic and useless from an engineering point of view. Therefore, a number of authors have tried to explain these infinities and have suggested ways to remove them.

Probably the first attempt in this direction was made by Staras [4]. He took the approach that this "infinity catastrophe" can be overcome by considering dipoles of non-zero dimension. Following Staras, Seshadri [5] found the functional form of the dependence of the radiation resistance on the antenna length. The radiation resistance varies as the reciprocal of the antenna length, and thus approached infinity as the antenna length approached zero. The source of the infinity was found to be the plasma resonance.

The magnetoionic theory has been used for predicting antenna properties in an anisotropic plasma without questioning its validity. Because of linearization in this theory the anisotropic plasma medium is resonant in some critical directions, where the wave number is infinite for certain operating frequencies of the antenna. In these critical directions the linearization process is not valid. Therefore, the use of the usual cold plasma dielectric tensor based on this linear theory is not right in the resonant regions.

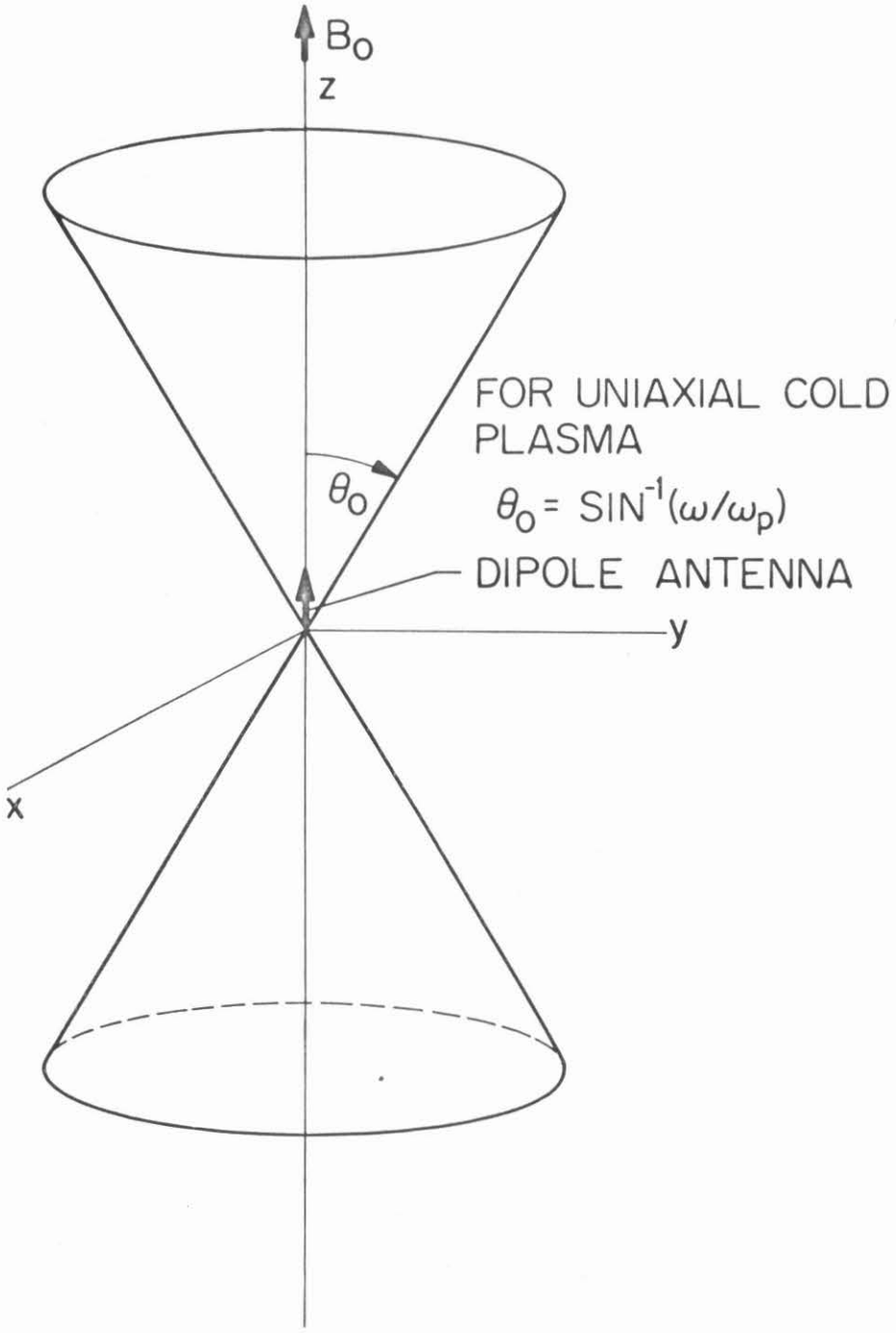

Figure 1.1 Diagram showing the cones in the field pattern of a small antenna at the origin. The semicone angle θ_o is determined by the plasma frequency ω_p, the operating frequency ω, and the cyclotron frequency.

Now if one considers the non-zero length ℓ of the dipole, only wave numbers $k < 1/\ell$ make sizable contributions to the radiation resistance. Hence if one chooses a long enough antenna, the contribution to the radiation resistance from the values of k near the critical directions can be considerably reduced, and hence the question of seriousness of the nonvalidity of the dielectric tensor near the critical directions can be disregarded.

Another attempt at resolving the "infinity catastrophe" has been made by Lee and Papas [6] . They suggested a new method for calculating the radiation resistance. Specifically, they claimed that the radiated power from an antenna in a magnetoplasma is not necessarily given by the conventional relation:

$$P = -\frac{1}{2} \mathrm{Re} \int_V \underline{J}^* \cdot \underline{E}_{out} \, dV$$

but rather is given by

$$P = -\frac{1}{4} \mathrm{Re} \int_V \underline{J}^* \cdot (\underline{E}_{out} - \underline{E}_{in}) \, dV$$

In the above formulas the subscripts "in" and "out" refer to the incoming (advanced) and outgoing (retarded) waves, respectively. By this new approach they claim to obtain a finite value for the radiation resistance of a point dipole in an anisotropic plasma.

The merits and demerits of the work of Lee and Papas are not yet well understood. Even if the infinity in radiation resistance does not appear, whether due to the contention of Staras and Seshadri, or to the

new approach of Lee and Papas, considerations of the more physical nature of the problem will introduce further modification in the calculation of the radiation resistance and the fields. In this paper we consider a more realistic problem and study the effects of electron thermal motion on the radiation characteristics of a short dipole antenna.

When the plasma can be considered to be isotropic, it is possible to obtain solutions of the hot plasma equations and study the effects of Landau damping [7] and compressibility [8] on the radiation resistance and the fields of an antenna. In the presence of a magnetostatic field the mathematics become involved and therefore this problem has received very little attention. To the author's knowledge, the first work done on this problem was by Deschamps and Kesler [9]. They studied the problem in the fluid model of the plasma and derived a formula for the radiation field of an arbitrary antenna. Chen [10] has also investigated this problem in the fluid model of the plasma and derived dyadic Green's function and a formula for the radiated power. Some aspects of this problem are studied by Tunaley and Grard [11] in the electrostatic approximation. In their paper they are right in noting that, in the electrostatic approximation, the phase velocity is infinite on a cone of half-cone angle $\cos^{-1}(\omega/\omega_p)$ in a uniaxial plasma. But they are wrong in concluding that these cones are those along which the electric field tends to infinity in the cold collisionless plasma. As a matter of fact, fields go to infinity on the cone of the half angle $\sin^{-1}(\omega/\omega_p)$.

In this paper the radiation characteristics of a short dipole antenna in a hot uniaxial plasma are studied. The uniaxial plasma is an approximation for large magnetic field $\underline{B}_o$ and small operating and plasma frequencies. Still we ignore the sheath around the dipole to make the problem tractable. The ion motions have been neglected. The fluid, as well as kinetic theory models of the plasma, are considered.

The input and radiation resistances of a dipole oriented parallel to the d.c. magnetic field $\underline{B}_o$ are studied in Chapter VII. It is found that in the fluid model of the plasma the resistances are always finite. Input resistance is studied as a function of the dipole length. Effect of Landau damping on the input and the radiation resistances is discussed.

The far fields have been evaluated by asymptotic methods in Chapter V. It is found that for $\omega < \omega_p$ the dipole excites two waves propagating within a cone, whose cone angle is slightly less than $\sin^{-1}(\omega/\omega_p)$. For $\omega > \omega_p$ there are three propagating waves. One of the waves corresponds to electromagnetic mode of radiation, while the other two waves are a hot plasma effect and correspond to a hot plasma mode of radiation. The radiation in the hot plasma mode is confined within a cone, whose axis is parallel to $\underline{B}_o$, and whose cone angle is determined by (ω/ω_p), and the electron thermal velocity V_o.

In Chapter VI near fields have been studied numerically. An interference structure is found in the angular distribution of the field patterns. The effects of antenna length ℓ, electron thermal

velocity, collisional and Landau damping on the near field patterns have also been investigated. The appearance of the interference structure in the angular distribution of the field pattern has been experimentally verified by Fisher [12].

Radiation conditions for solving Maxwell's equations are discussed in Chapter IV, while Chapter III deals with the velocities of the phase and the group propagation. It is found that for $\omega < \omega_p$ the radial power flow is in the opposite direction to the radial phase propagation. For $\omega > \omega_p$ the hot plasma mode has similar characteristics.

In Chapter II the problem has been formulated in kinetic and fluid models of the plasma. Equations for the field components are derived.

Chapter VIII has been devoted to studying the radiation characteristic of a dipole oriented perpendicular to the magnetic field $\underline{B}_o$.

In the last chapter some concluding remarks are made. Here some of the areas of further research and unsolved problems are singled out.

II. FORMULATION OF THE PROBLEM AND THE BASIC EQUATIONS

We consider an infinite and homogeneous plasma biased with an infinite external d.c. magnetic field $\underline{B}_o$ in the z-direction of the rectangular coordinate system. Geometry of the problem is shown in Figure 2.1. Filamentary dipole of length 2ℓ is assumed to be oriented parallel to the magnetic field $\underline{B}_o$. The current density on the antenna is given by

$$\underline{J}_s(\rho,z) = \frac{\delta(\rho)}{2\pi\rho} J_s(z)\, \underline{e}_z$$

where $\underline{e}_z$ is the unit vector parallel to the z direction. $J_s(z)$ gives the current distribution. Later on for getting some quantitative results, it is assumed to be triangular.

In order to treat the problem, plasma and Maxwell equations are solved with steady state time dependence $e^{-i\omega t}$. The field quantities obey Maxwell's equations, i.e.,

$$\nabla \times \underline{E} = +i\omega\mu_o \underline{H} \tag{2.2}$$

$$\nabla \times \underline{H} = \underline{J} - i\omega\varepsilon_o \underline{E} \tag{2.3}$$

$$\nabla \cdot \underline{E} = \rho/\varepsilon_o \tag{2.4}$$

$$\nabla \cdot \underline{B} = 0 \tag{2.5}$$

where $\underline{J}$ is the total current given by

$$\underline{J} = \underline{J}_s + \underline{J}_p$$

$\underline{J}_p$ is the induced plasma current. ρ and $\underline{J}$ are connected by the continuity equation $\nabla \cdot \underline{J} = i\omega\rho$. The foregoing equations can be

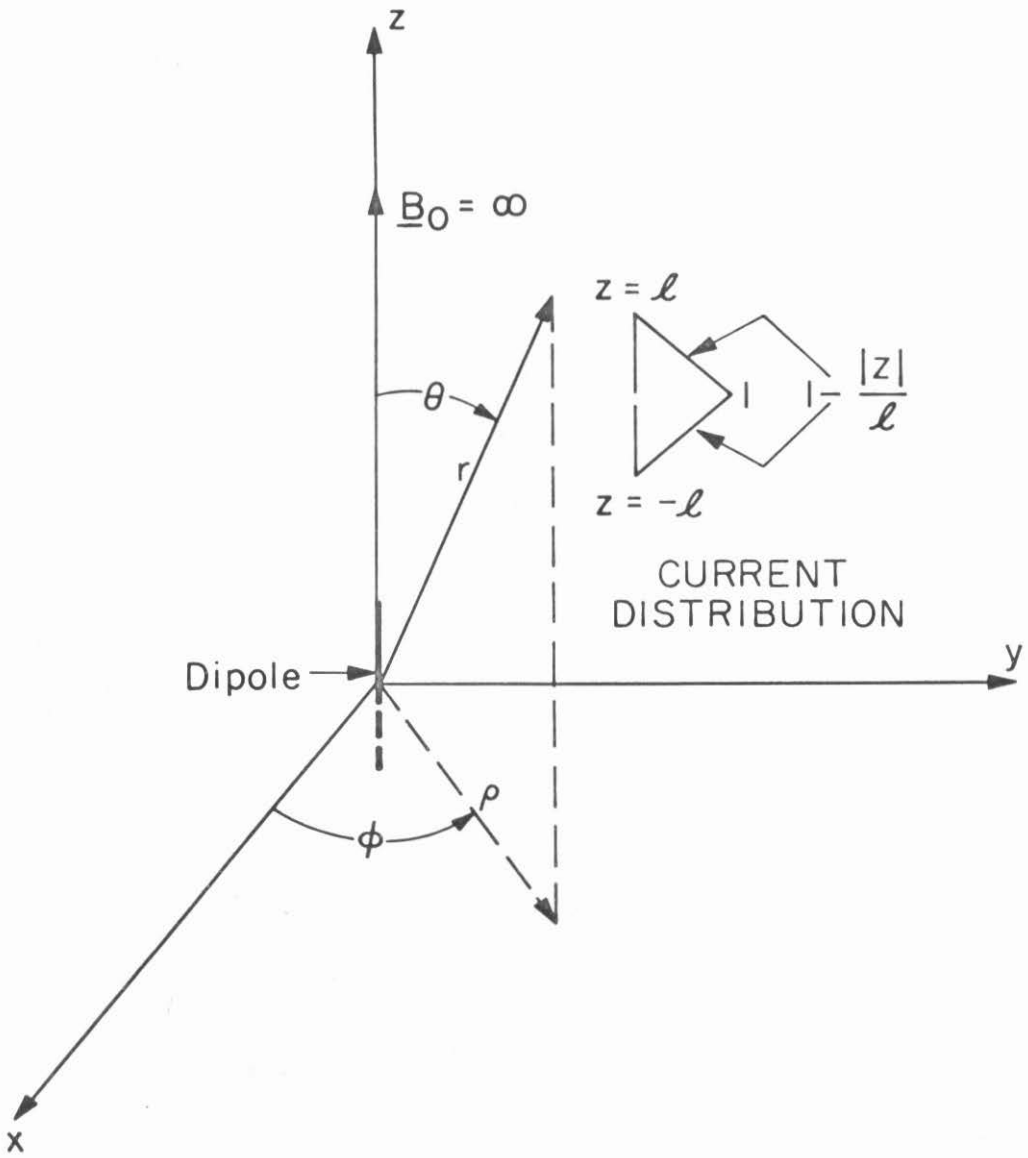

Figure 2.1 Geometry of the problem.

combined to give

$$\nabla^2 \underline{E} + \omega^2 \mu_o \varepsilon_o \underline{E} = -i\omega\mu_o \underline{J} - \frac{i}{\omega\varepsilon_o} \nabla\nabla \cdot \underline{J} \tag{2.6}$$

Since $\underline{B}_o$ is very large electron motion is confined along B_o and $\underline{J}_p$ has only one component i.e., $\underline{J}_p = J_p \underline{e}_z$. Next we derive expressions for $\underline{J}_p$ for both the fluid and the kinetic theory models of the plasma.

a) Fluid Model

In the fluid model the plasma current is given by

$$\underline{J}_p = -e\, n_o\, V_z\, \underline{e}_z \tag{2.7}$$

where n_o is the zero order electron density and V_z is the solution of the linearized plasma equation

$$-i\omega m_e \underline{V}_z = -e\, \underline{E}_z + i\, \frac{3\kappa T_e}{\omega}\, \frac{\partial^2 \underline{V}_z}{\partial z^2} - m_e \nu\, \underline{V}_z \tag{2.8}$$

m_e and T_e are the electron mass and temperature, respectively. κ is the Boltzmann constant. ν is the effective collision frequency. In arriving at equation (2.8) the equation of state for an adiabatic gas in one dimensional compression $p = 3n_e \kappa T_e$ has been used. The quantities n_e and p are the first-order perturbation in the electron density and the pressure respectively.

Solving equations (2.7) and (2.8) by taking Fourier transform with respect to z, we obtain

$$\hat{J}_p(\rho, k_z) = i\omega\varepsilon_o \frac{\omega_p^2}{\omega^2\left(1 + i\,\frac{\nu}{\omega}\right) - k_z^2 V_s^2}\, \hat{E}_z(\rho, k_z) \tag{2.9}$$

where a variable $\hat{g}(k_z)$ is the Fourier transform of $g(z)$ given by

$$\hat{g}(k_z) = \int_{-\infty}^{\infty} g(z)\, e^{-ik_z z}\, dz$$

and ω_p is the plasma frequency ($\omega_p^2 = \frac{n_o e^2}{m_e \varepsilon_o}$) and $V_s = \sqrt{\frac{3\kappa T_e}{m_e}}$.

Equation (2.9) can be written in the form

$$\hat{J}_p(\rho, k_z) = \frac{\omega \varepsilon_o}{i} (K_{||} - 1)\, \hat{E}_z(\rho, k_z) \tag{2.10}$$

where

$$K_{||} = 1 - \frac{\omega_p^2}{\omega^2 (1 + i\, \frac{\nu}{\omega}) - k_z^2 V_s^2} \tag{2.11}$$

b) Kinetic Theory Model

In kinetic theory model of the plasma to find the plasma current one solves the Vlasov equation for the electron distribution function F given by

$$\frac{\partial F}{\partial t} + \underline{V} \cdot \nabla F - \frac{e}{m_e} [\underline{E} + \underline{V} \times \underline{B}] \cdot \nabla_V F = 0 \tag{2.12}$$

For infinite magnetic field B_o it can be shown that

$$f = \int F\, dV_x\, dV_y$$

satisfies the following equation

$$\frac{\partial f}{\partial t} + V_z \frac{\partial f}{\partial z} - \frac{e}{m_e} E_z \frac{\partial f}{\partial V_z} = 0$$

Linearizing above equation by letting $f = f_o + f_1$, we find

$$\frac{\partial f_1}{\partial t} + V_z \frac{\partial f_1}{\partial z} - \frac{e}{m_e} E_z \frac{\partial f_o}{\partial V_z} = 0 \tag{2.13}$$

The current density J_p is given by

$$J_p = - en_o \int_{-\infty}^{\infty} f_1 V_z \, dV_z \tag{2.14}$$

Combining equations (2.13) and (2.14) we obtain for J_p

$$\hat{J}_p = -i\omega\varepsilon_o \frac{\omega_p^2}{k_z^2} \hat{E}_z \int_{-\infty}^{\infty} \frac{f_o / V_z}{V_z - \frac{\omega}{k_z}} \, dV_z \tag{2.15}$$

Then $K_{||}$ defined in (2.10) is given by

$$K_{||} = 1 - \frac{\omega_p^2}{k_z^2} \int_{-\infty}^{\infty} \frac{f_o / V_z}{(V_z - \frac{\omega}{k_z})} \, dV_z \tag{2.16}$$

For a Maxwellian velocity distribution $f_o(V_z) = \left(\frac{m_e}{2\pi\kappa T_e} \right)^{\frac{1}{2}} e^{- \frac{m_e V_z^2}{2\kappa T_e}}$

(2.16) can be written as

$$K_{||} = 1 - \frac{\omega_p^2}{k_z^2} Z'(\frac{\omega}{k_z V_o}) \tag{2.17}$$

where Z' is the derivative of the plasma distribution function [13] defined by

$$Z(t) = \pi^{-\frac{1}{2}} \int_{-\infty}^{\infty} \frac{e^{-x^2}}{(x-t)} \, dx \quad \text{and} \quad V_o = (\kappa T_e / m_e)^{\frac{1}{2}} = V_s / \sqrt{3}$$

Carrying out Fourier transform of (2.6) with respect to z and combining it with (2.10) we obtain for the z component of the electric field $\hat{E}_z(\rho, k_z)$

$$[\nabla_t^2 + \xi^2] \, E_z(\rho, k_z) = -i\omega\mu_o (1 - \frac{k_z^2}{k_o^2}) \hat{J}_s(k_z) \, \frac{\delta(\rho)}{2\pi\rho} \tag{2.18}$$

where ∇_t^2 is the transverse Laplacian, $k_o^2 = \omega^2 \mu_o \varepsilon_o$, and

$$\xi^2 = (k_o^2 - k_z^2) K_{||} \tag{2.19}$$

The other two nonzero field components are found in terms of E_z

$$\hat{E}_\rho(\rho, k_z) = \frac{ik_z}{k_o^2(1 - (k_z^2/k_o^2))} \frac{\partial}{\partial \rho} \hat{E}_z(\rho, k_z) \tag{2.20}$$

$$\hat{H}_\phi(\rho, k_z) = \frac{i}{\omega \mu_o (1 - (k_z^2/k_o^2))} \frac{\partial}{\partial \rho} \hat{E}_z(\rho, k_z) \tag{2.21}$$

Now (2.18) should be solved with proper radiation and boundary conditions. A physically reasonable radiation condition is to require that the fields should approach zero as ρ and z tend to infinity, and that the total radiated power from the antenna be positive. The consequences of this requirement will be seen later.

Poynting Vector Theorem for a Uniaxial Plasma

An energy conservation equation for the field quantities in a general medium is given by [14]

$$\nabla \cdot (\underline{E} \times \underline{H}^*) = - \underline{J}^* \cdot \underline{E} + i\omega(\mu_o \underline{H} \cdot \underline{H}^* - \varepsilon_o \underline{E} \cdot \underline{E}^*) \tag{2.22}$$

where $\underline{J}$ is the total current density. Since for the uniaxial plasma the plasma current is confined to the z direction, we have

$$\underline{J}^* \cdot \underline{E} = \underline{E} \cdot \underline{J}_s^* + \underline{E}_z \cdot \underline{J}_{zp}^* \tag{2.23}$$

where J_s is the current of any external source. For the fluid model

of the plasma, we obtain from equations (2.7) and (2.8)

$$E_z \cdot J_{zp}^* = i\omega\, m_e n_o V_z^* V_z + i\omega \frac{n_e^*}{n_o} n_e 3\kappa T_e + \nabla \cdot (\underline{e}_z 3\kappa T_e V_z^* n_e) \qquad (2.24)$$

Substituting the foregoing relation into (2.22) we obtain for the Poynting theorem for a uniaxial plasma

$$\nabla \cdot (\underline{E} \times \underline{H}^* + 3\underline{e}_z \kappa T_e V_z^* n_e) = -\underline{J}_s^* \cdot \underline{E} + i\omega[\mu_o \underline{H} \cdot \underline{H}^* - \varepsilon_o \underline{E} \cdot \underline{E}^* - m_e n_o V_z^* V_z + \frac{n_e^*}{n_o} n_e 3\kappa T_e] \qquad (2.25)$$

The above theorem is utilized in Chapter IV for calculating radiated power from the external current source. This will be used to determine the proper radiation condition for solving equation (2.18).

III. PHASE AND GROUP VELOCITIES IN A UNIAXIAL PLASMA

It is well known that in an anisotropic medium the direction of phase propagation differs, in general, from that of the energy propagation. The energy propagates with the group velocity. A detailed description of the phase and the group velocity in an anisotropic plasma is given by Holt and Haskel [15]. In this chapter we bring out some of the important features of the phase and group velocities and investigate how the electron temperature modifies them.

Figure 3.1 gives the orientations of the phase velocity $\underline{V}_p$, the group velocity $\underline{V}_g$ and the wave vector $\underline{k}$ for a plane wave of the form $e^{i(k\cdot r-\omega t)}$. The phase velocity $\underline{V}_p$ is parallel to $\underline{k}$ and its magnitude $V_p = c/\mu$, where c is the velocity of light in vacuum and μ is the refractive index defined by $\mu = \frac{c}{\omega} k$. The group velocity $\underline{V}_g$ is given by

$$\underline{V}_g = \frac{\partial \omega}{\partial \underline{k}} = \underline{e}_k \frac{\partial \omega}{\partial k} + \underline{e}_\psi \frac{1}{k} \frac{\partial \omega}{\partial \psi} \tag{3.1}$$

where $\underline{e}_k$ and $\underline{e}_\psi$ are the unit vectors parallel and normal to $\underline{k}$ respectively. ψ is the angle between $\underline{B}_o$ and $\underline{k}$. From (3.1) we find that the angle α between the phase and the group velocities is given by

$$\tan \alpha = \frac{1}{\mu} \frac{\partial \mu}{\partial \psi} \tag{3.2}$$

and the magnitude of the group velocity can be written as

$$V_g = \frac{c}{\frac{\partial}{\partial \omega}(\omega \mu) \cos \alpha} \tag{3.3}$$

The wave vector $\underline{k}$ is the solution of the dispersion relation for the medium. In this case the dispersion relation is obtained from equation (2.18) by setting its right hand side equal to zero and taking Fourier transform with respect to x and y. Thus we obtain

$$-k_x^2 - k_y^2 + (K_o^2 - k_z^2)\, K_{||} = 0 \tag{3.4}$$

where k_x and k_y are the Fourier transform variables with respect to x and y. Noting from Figure 3.1 that $\sqrt{k_x^2 + k_y^2} = k \sin\psi$, $k_z = k \cos\psi$ and substituting for $K_{||}$ the expression in (2.11) with $\nu = 0$ we obtain an equation for the wave number k

$$k^4 V_s^2 \cos^2\psi - k^2\omega^2 \left[1 + \cos^2\psi(\beta^2 - \frac{\omega_p^2}{\omega^2})\right] + \frac{\omega^2}{c^2}(\omega^2 - \omega_p^2) = 0 \tag{3.5}$$

where $\beta = V_s/c$. Solving this equation for $\mu = \frac{c}{\omega} k$ we have

$$\mu^2 = \frac{a \pm \sqrt{a^2 - 4\beta^2\cos^2\psi(1 - \frac{\omega_p^2}{\omega^2})}}{2\beta^2\cos^2\psi} \tag{3.6}$$

where $a = 1 + \cos^2\psi(\beta^2 - \frac{\omega_p^2}{\omega^2})$.

Cold Plasma

For a cold plasma $V_s = 0$ and so (3.5) becomes quadratic in $\mu = kc/\omega$ and yields directly

$$\mu = \left[\frac{\omega^2 - \omega_p^2}{\omega^2 - \omega^2\cos^2\psi}\right]^{1/2} \tag{3.7}$$

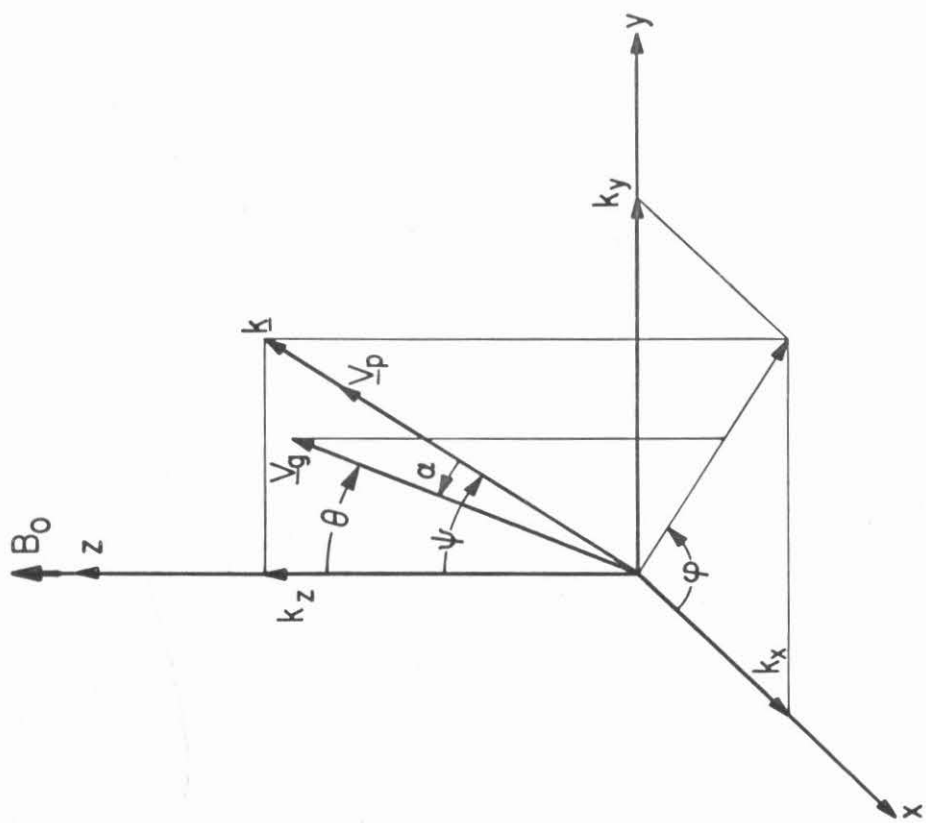

Figure 3.1 Orientations of phase velocity $\underline{V}_p$, group velocity $\underline{V}_g$ and wave vector $\underline{k}$ with respect to $\underline{B}_o$.

We can see from (3.7) that for $\omega > \omega_p$, μ is real for all values of ψ. For $\omega < \omega_p$, μ is real only for $0 < \psi < \cos^{-1}(\frac{\omega}{\omega_p})$. The value of $\psi = \psi_o = \cos^{-1}(\frac{\omega}{\omega_p})$ is the cone angle where the wave number is infinite and the phase velocity vanishes. For $\psi > \psi_o$ the waves are evanescent (k is imaginary).

From (3.2) and (3.7) we obtain after some algebra

$$\tan \alpha = \left(\frac{\omega_p \cos \psi \sin \psi}{\omega_p^2 \cos^2 \psi - \omega^2} \right) \tag{3.8}$$

Now when $\psi = \psi_o$, $\alpha = \pi/2$, i.e., group velocity vector makes an angle of 90° with the phase velocity vector. Also, at this angle it can be shown that the group velocity vanishes.

The angle θ which the group velocity makes with respect to B_o can be easily shown to be related to the angle ψ, the angle between the phase velocity and B_o, through the following relation

$$\tan \theta = \tan(\psi - \alpha) = - \frac{\omega^2}{\omega_p^2} \frac{\tan \psi}{1 - \frac{\omega^2}{\omega_p^2}} \tag{3.9}$$

For $\omega < \omega_p$, angle θ reaches its maximum value when $\psi = \cos^{-1}(\frac{\omega}{\omega_p})$, and this value is given by $\theta = \theta_o = -\sin^{-1}(\frac{\omega}{\omega_p})$. The two angles ψ_o and θ_o are thus complementary to one another. The values of θ given by (3.9) are negative, indicating that the radial component of the phase and group velocities are directed in opposite directions. Thus in the radial direction phase propagation is inward, while for $\omega > \omega_p$, θ is always positive and thus the radial component of the velocities are both outward. The upper plot in Figure 3.2 and Figure 3.3 give polar plots of

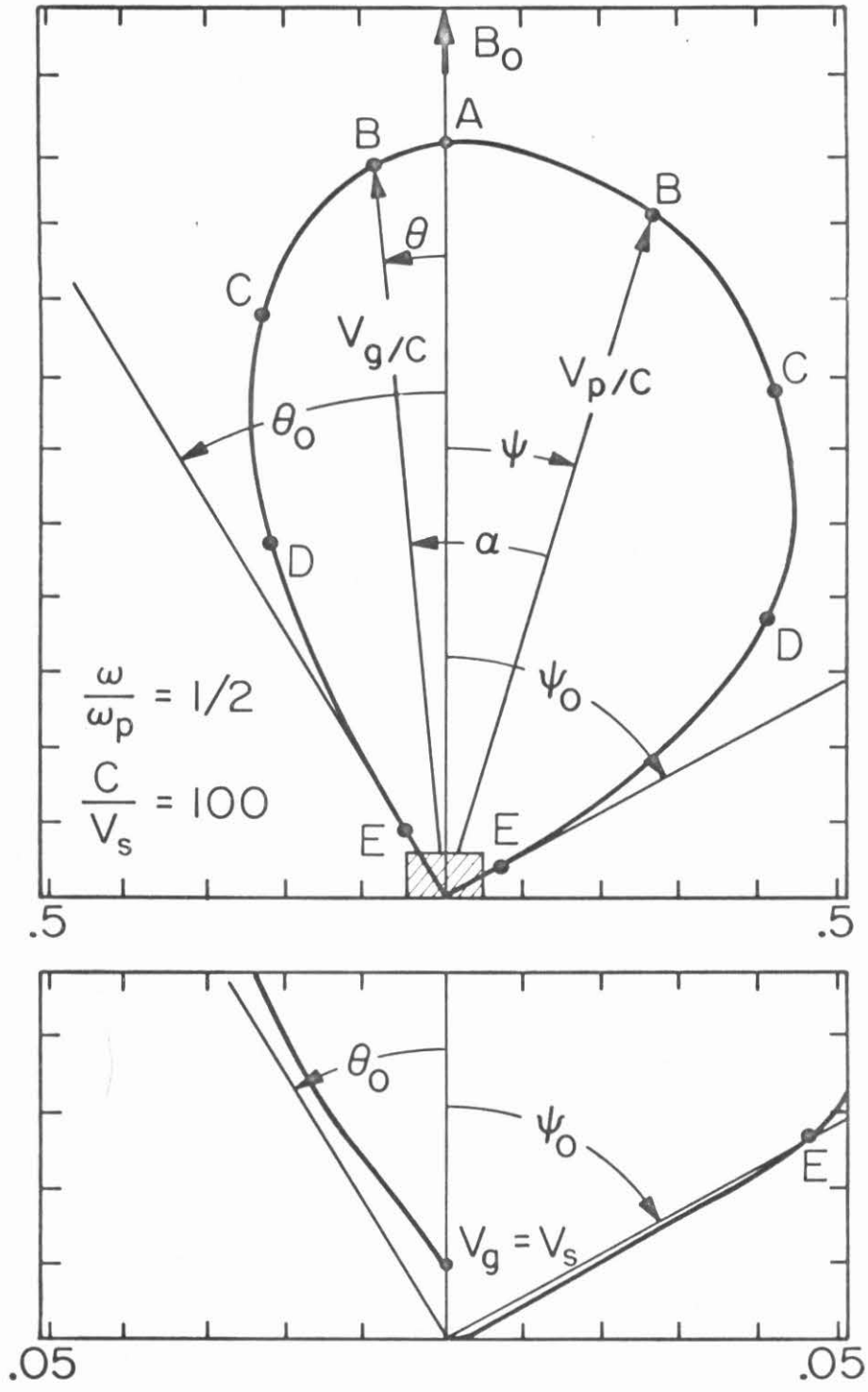

Figure 3.2 Polar plot of phase velocity (right side) and group velocity (left side) for $B_o = \infty$, $\omega_p/\omega = 2$. Lower plot shows shaded region, where electron thermal velocities are important, on an expanded scale.

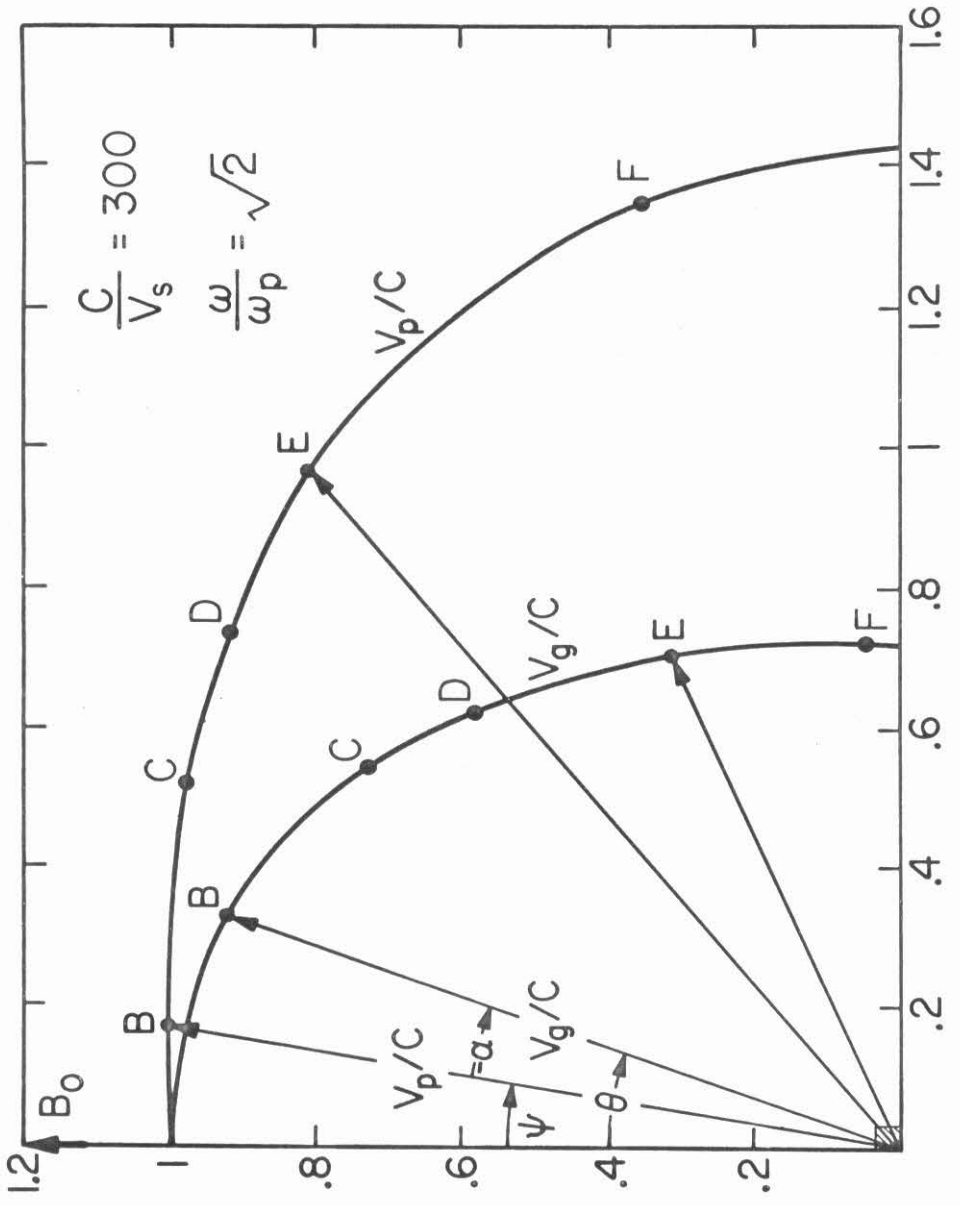

Figure 3.3 Phase and group velocity for the electromagnetic mode.

the phase and group velocities for $\omega < \omega_p$ and $\omega > \omega_p$, respectively. Only in the shaded region of the upper plot in Figure 3.2, hot plasma effects are important. These plots display above mentioned characteristics diagrammatically.

Since in a lossless plasma energy propagates along the group velocity, for $\omega < \omega_p$ the radiation from a source embedded in a uniaxial plasma will be confined within a cone of semicone angle $\theta_o = \sin^{-1}(\frac{\omega}{\omega_p})$ (Fig. 1.1). It should be emphasized here that θ_o can be greater or smaller than ψ_o depending upon the value of (ω/ω_p), since $\theta_o + \psi_o = \pi/2$. For $\omega > \omega_p$ all directions are allowed for V_g and hence the antenna will radiate in all directions.

Hot Plasma

In the case of a hot plasma, simple analytical relations like (3.8) and (3.9) cannot be obtained, but the polar plots of the phase and group velocities can easily be obtained numerically.

It can be easily seen that for $\omega < \omega_p$ only one of the two solutions in (3.6) gives real values of μ. For $\omega > \omega_p$ both the solutions give real values for μ. Thus for $\omega < \omega_p$ there is only one mode of propagation, while for $\omega > \omega_p$ there are two modes.

Case 1 $\omega < \omega_p$.

For this case effects of electron temperature are shown in the lower plot of Fig. 3.2. The lower plot shows the shaded region in the upper plot, where electron thermal velocities are important, on an expanded scale. For the hot plasma, the phase velocity has real values even beyond $\psi > \psi_o$. But still the group velocity has real values only

for $\theta < \theta_o$. For any angle $\theta < \theta_o$ the group velocity is now double valued. Gould and Fisher [16] have reported similar results. We will see in Chapter V that these two group velocities for any $\theta < \theta_o$ correspond to two propagating waves, a slow wave and a fast wave, within a cone of half-cone angles θ_o.

Case 2 $\omega > \omega_p$.

The solution in (3.6) with the minus sign gives a similar polar plot to that given in Fig. 3.3 for $\beta \ll 1$. The mode of propagation given by this solution is not much affected by the electron temperature unless β is large. For large values of β relativistic effects enter and our analysis would require some modification.

For the solution with positive sign in (3.5) polar plots for the group and phase velocities are given in Fig. 3.4. This mode of propagation is due to hot plasma effects. The group velocity of this model is confined within a small cone and is double valued within this cone. In Chapter V it will be seen that the two values of the group velocity correspond to two propagating waves in a hot plasma mode.

It should be noted that the preceding discussion of hot plasma effects was based on the fluid description of the plasma. In kinetic description of the plasma, the waves with phase velocities $V_p \sim V_o$ will be strongly damped because of Landau damping. Actual calculations of near zone fields and radiation and input resistances in later chapters will be made for both models.

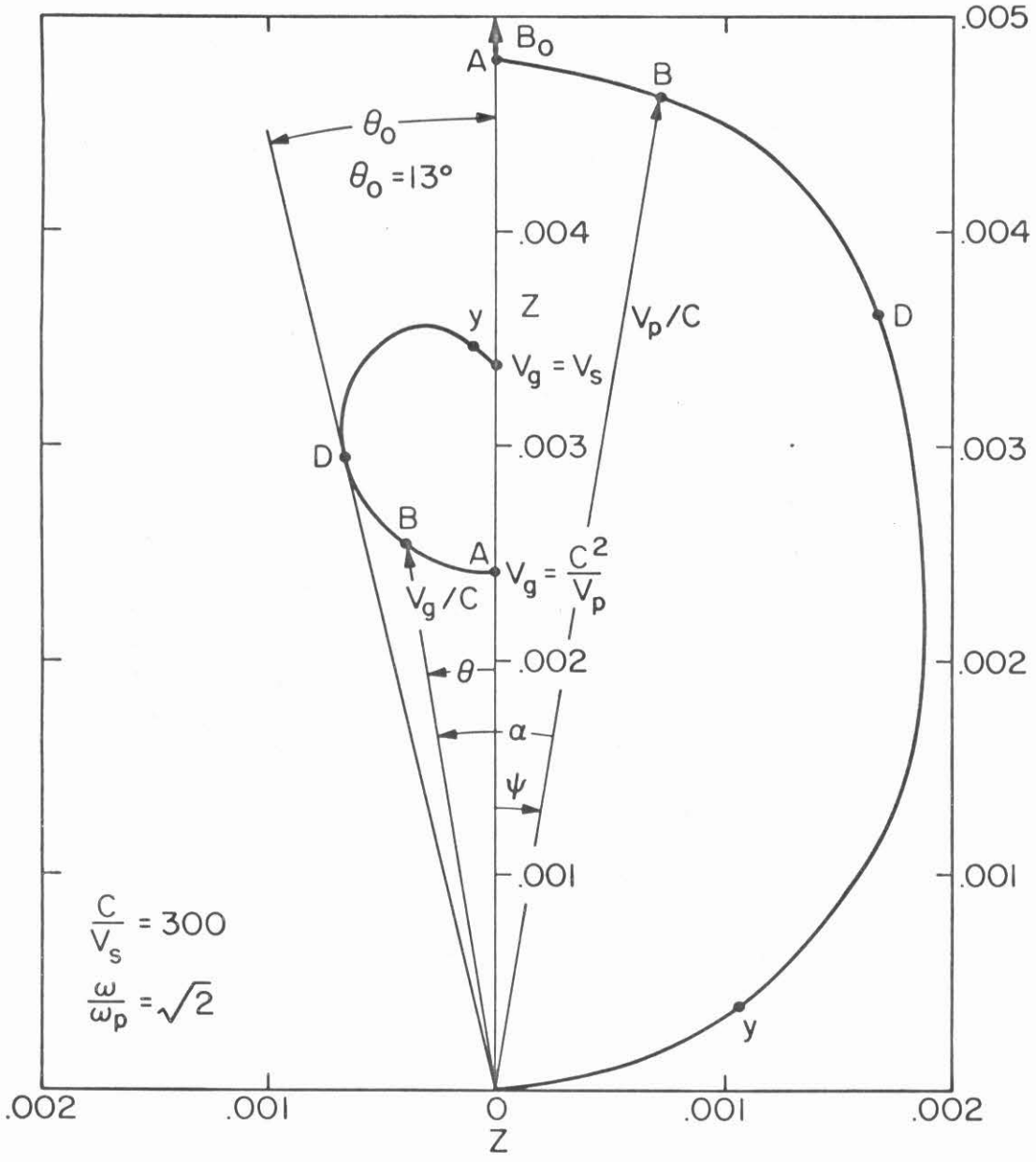

Figure 3.4 Polar plot of phase velocity (right side) and group velocity (left side) for the hot phase mode of radiation.

IV. RADIATION CONDITIONS AND THE INTEGRAL REPRESENTATION OF THE FIELDS

The purpose of this chapter is to solve the differential equation in (2.18) and choose one of the two possible solutions which gives outwardly directed power flow. It is found that in some cases radial phase propagation is in opposite direction to the radial power flow.

4.1 Expression for the Field Components and the Radiated Power

Equation (2.18) can be solved to give

$$E_z(\rho,k_z) = A(k_z)\, H_o^{(n)}(\xi\rho) \ , \qquad \rho > 0 \tag{4.1}$$

where $H_o^{(n)}(k_z)$ is the Hankel function of either the first or second kind ($n = 1$ or 2). $A(k_z)$ can be determined by the nature of the source by requiring that

$$\lim_{\rho \to 0} 2\pi\rho\, H_\phi = \hat{J}_s(k_z) \tag{4.2}$$

Substituting equation (4.1) into (2.21) we obtain

$$H_\phi(\rho,k_z) = -\frac{iA(k_z)}{\omega\mu_o\left(1-\frac{k_z^2}{k_o^2}\right)}\ \xi H_1^{(n)}(\xi\rho)$$

For the small argument formula for $H_1^{(n)}(\xi\rho)$, H_ϕ can be written

$$H_\phi(\rho,k_z) = (-1)^{n-1}\frac{A(k_z)}{\omega\mu_o\left(1-\frac{k_z^2}{k_o^2}\right)}\ \frac{2}{\pi\rho}$$

Hence we obtain from (4.2)

$$A(k_z) = (-1)^{n-1} \frac{\omega\mu_o}{4} \left(1 - \frac{k_z^2}{k_o^2}\right) \hat{J}_s(k_z) \quad .$$

Now the three field components $\hat{E}_z(\rho,k_z)$, $\hat{E}_\rho(\rho,k_z)$ and $\hat{H}_\phi(\rho,k_z)$ can be written

$$\hat{E}_z(\rho,k_z) = (-1)^{n-1} \frac{\omega\mu_o}{4} \left(1 - \frac{k_z^2}{k_o^2}\right) \hat{J}_s(k_z)\, H_o^{(n)}(\xi\rho) \tag{4.3a}$$

$$\hat{E}_\rho(\rho,k_z) = (-1)^{n} \frac{ik_z}{4\omega\,\varepsilon_o} \hat{J}_s(k_z)\, H_1^{(n)}(\xi\rho) \tag{4.3b}$$

$$\hat{H}_\phi(\rho,k_z) = (-1)^{n} \frac{i\xi}{4} \hat{J}_s(k_z)\, H_1^{(n)}(\xi\rho) \tag{4.3c}$$

The value of n in (4.3a) to (4.3c) is determined on the basis of which one gives outgoing power. Therefore, we next calculate the total radiated power. We use the Poynting theorem in (2.25). Considering a cylinder with z axis as its axis, and of radius ρ and height $2h$ (Fig. 4.1) and integrating both sides of equation (2.25) on this cylindrical volume, we obtain

$$-2\pi\rho \frac{1}{2} \mathrm{Re} \int_{-h}^{h} E_z H_\phi^* \, dz + 2\pi\rho \,\mathrm{Re} \int_0^\rho [E_\rho \, H_\phi^*]_{z=h} \, d\rho$$

$$+ 2\pi\rho \,\mathrm{Re} \int_0^\rho \kappa T_e \, [V_z^* \, n_e]_{z=h} \, d\rho = -\frac{1}{2} \mathrm{Re} \int_V \underline{J}_s^* \cdot \underline{E} \, dV \tag{4.5}$$

Assuming that as h tends to infinity the fields are zero so that the second and third terms on the left side vanish, we obtain

$$-2\pi\rho \frac{1}{2} \text{Re} \int_{-\infty}^{\infty} E_z H_\phi^* \, dz = -\frac{1}{2} \text{Re} \int_V \underline{J}_s^* \cdot \underline{E} \, dV \tag{4.6}$$

The right hand side of the above equation is the time average input power and the left hand side is the time average radiated power. Here essentially it has been shown that in a lossless plasma the total input and the radiated power are equal. Denoting the total time average radiated power by P we have

$$P = -2\pi\rho \frac{1}{2} \text{Re} \int_{-\infty}^{\infty} E_z(\rho,z) \, H_\phi^*(\rho,z) \, dz \tag{4.7}$$

Applying Parseval's theorem to (4.7) and using equations (4.3a) and (4.3c) we obtain for P

$$P = \frac{\omega\mu_o}{16} \rho \, \text{Im} \int_0^{\infty} dk_z \left(1 - \frac{k_z^2}{k_o^2}\right) \hat{J}_s^2(k_z) \xi^* \, H_o^{(n)}(\xi\rho) \, H_1^{(n)*}(\xi\rho) \tag{4.8}$$

For the collisionless fluid model of the plasma ξ is either pure real or pure imaginary. In that case the above expression for P can be simplified. The Wronskian relation for the Hankel function gives

$$H_1^{(1)}(\xi\rho) \, H_o^{(2)}(\xi\rho) - H_o^{(1)}(\xi\rho) \, H_1^{(2)}(\xi\rho) = \frac{-4i}{\pi\xi\rho}$$

If ξ is pure real then remembering that $H_\nu^{(1)*}(\xi\rho) = H_\nu^{(2)}(\xi\rho)$ we have

$$\text{Im}[\xi^* H_o^{(n)}(\xi\rho) \, H_1^{(n)*}(\xi\rho)] = (-1)^{n-1} \frac{2}{\pi\rho}$$

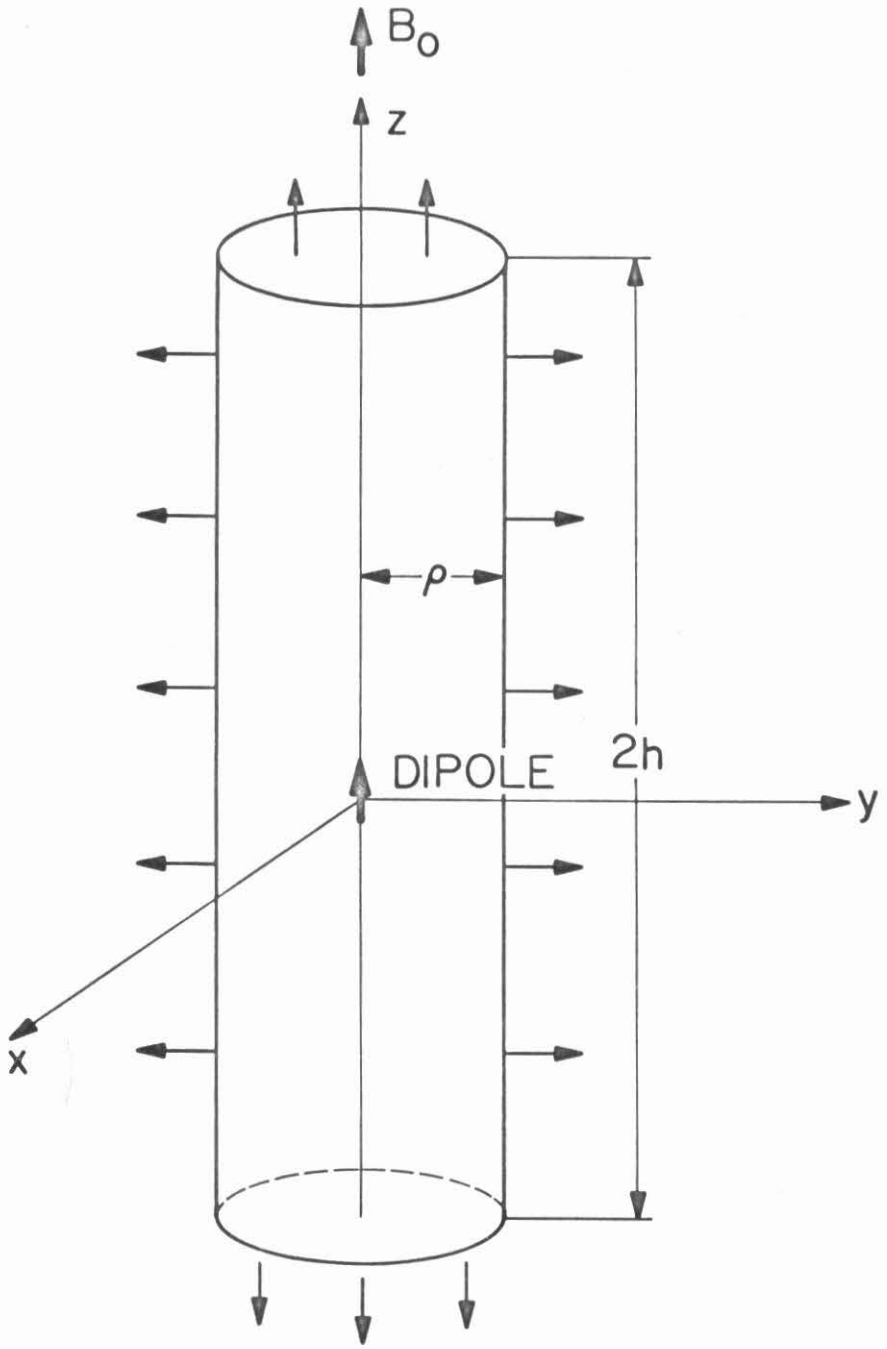

Figure 4.1 Cylindrical volume for calculating radiated power.

when ξ is pure imaginary; then using the relation

$$k_\nu(a) = (-1)^{n-1}\, \pi i\, e^{i\nu\pi/2}\, H^{(n)}((-1)^{n-1} ia)$$

it can be easily shown that

$$\mathrm{Im}\,[\xi^*\, H_o^{(n)}(\xi\rho)\, H_1^{(n)*}(\xi\rho)] = 0$$

Therefore we have

$$\mathrm{Im}\,[\xi^*\, H_o^{(n)}(\xi\rho)\, H_1^{(n)*}(\xi\rho)] = \begin{cases} (-1)^{n-1}\, \dfrac{2}{\pi\rho} & \text{Real } \xi \\ 0 & \text{Im } \xi \end{cases} \tag{4.9}$$

and

$$P = \frac{\omega\mu_o}{8\pi}\,(-1)^{n-1} \int_{\text{Real } \xi} dk_z \left(1 - \frac{k_z^2}{k_o^2}\right) \hat{J}_s^2(k_z) \tag{4.10}$$

where $\int_{\text{Real } \xi}$ denotes that the integral is to be evaluated only for those of k_z for which ξ is real. This expression for the power demonstrates that the contribution to the radiated power comes only from the real value of ξ. Also, only these real values of ξ give propagating waves. To find the right value of n in (4.10) so that P is positive, giving outwardly directed power flow, we treat the cases $\omega < \omega_p$ and $\omega > \omega_p$ in the next two sections.

4.2 Case $\omega < \omega_p$

For the collisionless fluid model of the plasma ξ is given by the equations (2.11) and (2.19) with $\nu = 0$. It can be easily seen that ξ is real when $k_o < k_z < \omega/V_s$ and it is imaginary otherwise.

Therefore (4.10) can be written

$$P = \frac{\omega\mu_o}{8\pi} (-1)^{n-1} \int_{k_o}^{\omega/V_s} dk_z \left(1 - \frac{k_z^2}{k_o^2}\right) \hat{J}_s^2(k_z)$$

The integrand in the above integral is negative. In order to make P always positive so that the power flow is outwardly directed, we must choose $n = 2$. Therefore, we obtain

$$P = \frac{\omega\mu_o}{8\pi} \int_{k_o}^{\omega/V_s} \left(\frac{k_z^2}{k_o^2} - 1\right) \hat{J}_s^2(k_z)\, dk_z \tag{4.11}$$

$$\hat{E}_z(\rho,k_z) = -\frac{\omega\mu_o}{4} \left(1 - \frac{k_z^2}{k_o^2}\right) \hat{J}_s(k_z)\, H_o^{(2)}(\xi\rho) \tag{4.12a}$$

$$\hat{E}_\rho(\rho,k_z) = \frac{ik_z\xi}{4\omega\varepsilon_o} \hat{J}_s(k_z)\, H_1^{(2)}(\xi\rho) \tag{4.12b}$$

$$\hat{H}_\phi(\rho,k_z) = \frac{i\xi}{4} \hat{J}_s(k_z)\, H_1^{(2)}(\xi\rho) \tag{4.12c}$$

Since 4.13a, b, and c involve the Hankel function of the second kind, the phase propagation is inward and in the opposite direction to that of the radial power flow. Similar behavior is noted by Seshadri [17] in the case of a cold plasma. This implies that the radial components of the group and phase propagation are directed in opposite directions. Indeed this is true, as is evident from Figure 3.2.

4.3 Case $\omega > \omega_p$

In this case ξ is real in two regions $0 < k_z < k_o$ and $\frac{\omega}{V_s}\sqrt{1 - \frac{\omega_p^2}{\omega^2}} < k_z < \frac{\omega}{V_s}$ provided $\frac{\omega_p}{\omega} < \sqrt{1 - \frac{V_s^2}{c^2}}$. Hence the total radiated power given by equation (4.10) can be written

$$P = \frac{\omega\mu_o}{8\pi}(-1)^{n-1}\int_0^{k_o}(1 - \frac{k_z^2}{k_o^2})\,\hat{J}_s^2(k_z)\,dk_z$$

$$+ \frac{\omega\mu_o}{8\pi}(-1)^{n-1}\int_{\frac{\omega}{V_s}\sqrt{1-\frac{\omega_p^2}{\omega^2}}}^{\omega/V_s}(1 - \frac{k_z^2}{k_o^2})\,\hat{J}_s^2(k_z)\,dk_z \qquad (4.13)$$

When $\omega_p = 0$ the foregoing expression for the power should reduce to the free space case. In that case the second term is zero and only the first term contributes to the total power. Denoting this power by P_{fs} we have

$$P_{fs} = \frac{\omega\mu_o}{8\pi}(-1)^{n-1}\int_0^{k_o}(1 - \frac{k_z^2}{k_o^2})\,\hat{J}_s^2(k_z)\,dk_z \qquad (4.14)$$

The integrand in (4.14) is always positive. Therefore to make P_{fs} positive we must choose $n = 1$. In the electrostatic approximation ($\mu_o = 0$) the first term in (4.13) vanishes and then the expression for the power becomes

$$P = -(-1)^{n-1}\frac{1}{8\pi\omega\varepsilon_o}\int_{\frac{\omega}{V_s}\sqrt{1-\frac{\omega_p^2}{\omega^2}}}^{\omega/V_s} k_z^2\,\hat{J}_s^2(k_z)\,dk_z$$

In order that the power be outwardly flowing in the electrostatic approximation, we choose $n = 2$. Therefore radiation conditions for $\omega > \omega_p$ are $n = 1$ for $0 < k_z < k_o$ and $n = 2$ for $\frac{\omega}{V_s}\sqrt{1-\frac{\omega_p^2}{\omega^2}} < k_z < \frac{\omega}{V_s}$. This gives two distinct modes of propagation. The two terms in (4.13) correspond to these two modes. In the mode for which $H_o^{(1)}(\xi\rho)$ is the permissible solution, the radial phase and group velocities point in the same direction. For the other mode for which $H_o^{(2)}(\xi\rho)$ is the permissible solution, the radial phase propagation is inward. These facts are clearly demonstrated by Figures 3.3 and 3.4.

Now knowing the proper choice of n, the behavior of fields as functions of space coordinates can be found by taking the Fourier inverse transform of the equations 4.3a,b,c, i.e.,

$$E_z(\rho,z) = (-1)^{n-1}\frac{\omega\mu_o}{8\pi}\int_{-\infty}^{\infty}\left(1-\frac{k_z^2}{k_o^2}\right)\hat{J}_s(k_z)\,H_o^{(n)}(\xi\rho)\,e^{ik_z z}\,dk_z \quad (4.15a)$$

$$E_\rho(\rho,z) = (-1)^{n}\frac{i}{8\omega\,\varepsilon_o\pi}\int_{-\infty}^{\infty} k_z\xi\,\hat{J}_s(k_z)\,H_1^{(n)}(\xi\rho)e^{ik_z z}\,dk_z \quad (4.15b)$$

$$H_\phi(\rho,z) = (-1)^{n}\frac{i}{8\pi}\int_{-\infty}^{\infty}\xi\,\hat{J}_s(k_z)\,H_1^{(n)}(\xi\rho)\,e^{ik_z z}\,dk_z \quad (4.15c)$$

The evaluation of the integrals in the foregoing will give the behavior of fields in space. This is the subject matter of the next two chapters.

V. FAR FIELDS

This chapter is devoted to finding the asymptotic representation of the fields for large values of r $(r = \sqrt{\rho^2 + z^2})$. For $\omega < \omega_p$ it is found that the dipole excites two propagating waves, a slow wave and a fast wave. These waves propagate only within a cone. Near the cone surface the field components can be represented by the Airy function. When $\omega > \omega_p$ the dipole excites three propagating waves. One of the waves is similar to the wave excited by a dipole in free space. Therefore we call this wave the electromagnetic mode of radiation. The other two waves are hot plasma effects and propagate only within a cone. The field consisting of these two waves has been called radiation into a hot plasma mode.

Here we will find asymptotic representation for E_z only. Similar expressions can be obtained for E_ρ and H_ϕ. Rewriting (4.15a) we have

$$E_z(\rho,z) = (-1)^{n-1} \frac{\omega\mu_o}{8\pi} \int_{-\infty}^{\infty} \left(1 - \frac{k_z^2}{k_o^2}\right) \hat{J}_s(k_z)\, H_o^{(n)}(\xi\rho)\, e^{ik_z z}\, dk_z \tag{5.1}$$

It is convenient to introduce the spherical coordinate system through

$$\rho = r \sin\theta \qquad \text{and} \qquad z = r\cos\theta \quad , \quad r > 0$$

For waves propagating in the positive z direction, angle θ is in the range $0 < \theta < \pi/2$. If r is large the argument of the Hankel function $(\xi\rho)$ can be likewise made large if ξ and $\sin\theta$ are not

zero. In that case the Hankel function can be replaced by its asymptotic expansion, i.e.,

$$H_o^{(n)}(\xi r \sin\theta) \simeq \left(\frac{2}{\pi r \sin\theta}\right)^{1/2} e^{(-1)^{n-1} i \left[\xi r \sin\theta - \frac{\pi}{4}\right]} \tag{5.2}$$

ξ is given by equation (2.19). $K_{||}$ is never zero for the kinetic model of the plasma and for the fluid model $K_{||}$ is always nonzero only when collisions are included. Hence ξ has only zeros at $k_z = \pm k_o$. But the integrand in (5.1) vanishes at $k_z = k_o$. Therefore in equation (5.1) the contribution to the integral from the vicinity of $k_z = k_o$ is negligible and E_z can be approximated by

$$E_z(r,\theta) \simeq (-1)^{n-1} \frac{\omega\mu_o}{4\pi\sqrt{2\pi r \sin\theta}} e^{(-1)^n i \frac{\pi}{4}} \int_{-\infty}^{\infty} F(k_z)\, e^{irQ(k_z,\theta)}\, dk_z \tag{5.3}$$

where

$$F(k_z) = \frac{\hat{J}_s(k_z)\left(1 - \frac{k_z^2}{k_o^2}\right)}{\sqrt{\xi}} \tag{5.4}$$

and

$$Q(k_z,\theta) = (-1)^{n-1}\xi \sin\theta + k_z \cos\theta \tag{5.5}$$

The asymptotic expression for the integral in (5.3) can be obtained by the method of stationary phase [18] . The main contribution to the integral comes from small regions near the stationary points given by

$$\frac{dQ(k_z,\theta)}{dk_z} = 0 \quad \text{or} \quad \xi'(k_z) = (-1)^n \cot\theta \ , \quad 0 < \theta < \frac{\pi}{2} \tag{5.6}$$

where the prime denotes d/dk_z .

Now in the following two sections the two cases $\omega < \omega_p$ and $\omega > \omega_p$ are considered.

5.1 Case $\omega < \omega_p$

We recall from Chapter IV that we must choose $n = 2$ for $\omega < \omega_p$ in order that the power flow be outwardly directed. Then we can write equations (5.3) and (5.6) as

$$E_z(r,\theta) \simeq - \frac{\omega\mu_o}{4\pi\sqrt{2\pi r \sin\theta}} e^{i\frac{\pi}{4}} \int_{-\infty}^{\infty} F(k_z)\, e^{irQ(k_z,\theta)}\, dk_z \tag{5.7}$$

$$\xi'(k_z) = \cot\theta \tag{5.8}$$

In the collisionless fluid model of the plasma ξ is pure real for some part of the real k_z axis and pure imaginary for the rest of it. For $\omega < \omega_p$ even in the collisionless limit $K_{||}$ is never zero. Hence the representation of the field by (5.7) is still valid. There may be stationary points on the real k_z axis. These can be found by plotting θ against k_z from equation (5.8) as shown in Figure 5.1.

Only real stationary points for which $\xi(k_{zi})$ is also real will contribute to the radiation in the far zone. For fluid model of the plasma ξ is real only when $k_o < |k_z| < \omega/V_s$. For $0 < \theta < \frac{\pi}{2}$, $\cot\theta$ is positive. It can be seen from equations (2.11) and (2.19) that ξ'

is positive only for positive values of k_z . Therefore only positive stationary points contribute to waves propagating for $0 < \theta < \frac{\pi}{2}$.

It is interesting to note from Figure 5.1 that for any angle θ less than θ_o there are <u>two real stationary points</u>. There are no real stationary points for $\theta > \theta_o$. At $\theta = \theta_o$ the two stationary points coalesce. The two real stationary points for $\theta < \theta_o$ give rise to two propagating waves within the cone (Figure 1.1) of half-cone angle θ_o . Outside the cone the waves are evanescent. If we now refer back to Figure 3.2, we see that θ_o is the same half-cone angle beyond which the group velocity has no real value. Within the cone the two group velocities for any θ correspond to these two waves.

Now knowing locations and the nature of the stationary points asymptotic expressions for the fields can be obtained inside the cone ($\theta < \theta_o$), on the cone ($\theta \simeq \theta_o$) and outside the cone ($\theta > 0_o$).

5.1.1 Fields inside the Cone

Inside the cone the two stationary points contribute separately to the field. Since most significant contributions to the integral come from the neighborhood of the stationary points, the range of integration may be reduced to two short segments centered at k_{z1} and k_{z2} (Figure 5.1), respectively. In each segment $Q(k_z,\theta)$ may be approximated by the first three terms of its Taylor expansion, whereas the remaining factor $F(\lambda)$, being a slowly varying function of k_z , may be approximated by its value at k_{z1} and k_{z2} ; thus

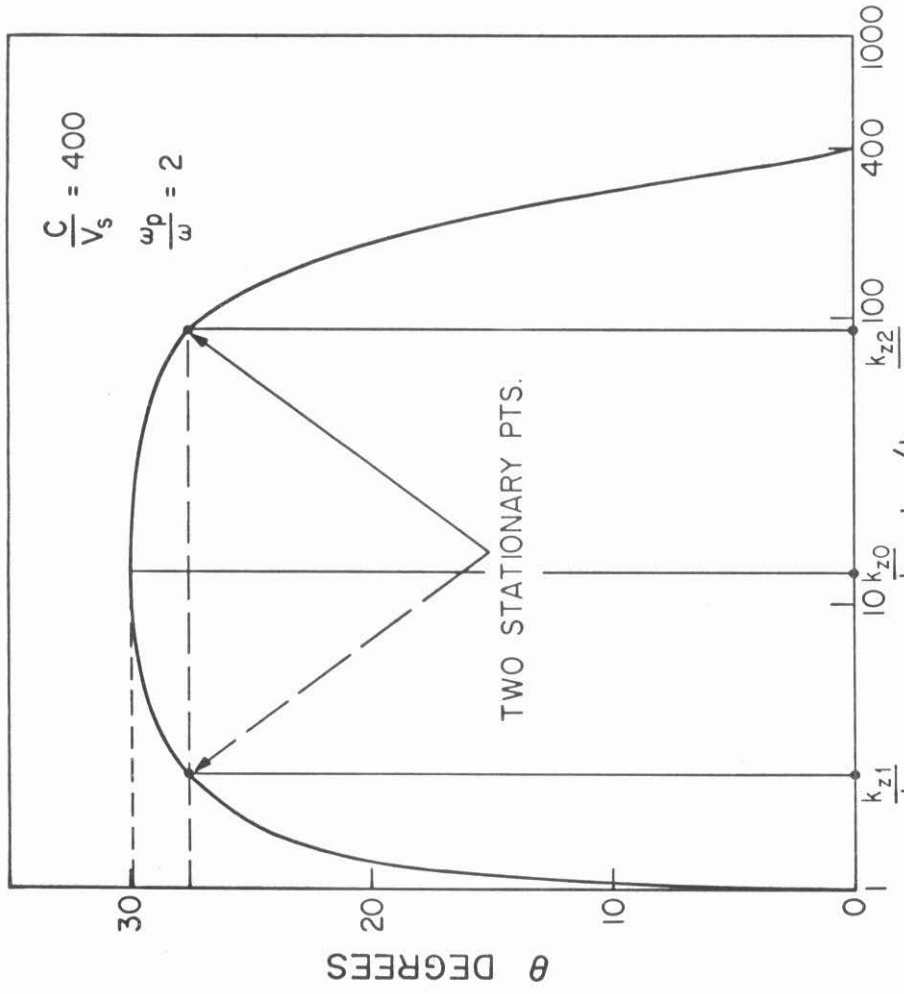

Figure 5.1 Stationary point plot for $\omega < \omega_p$

$$Q(\lambda,\theta) = \begin{cases} Q(k_{z1},\theta) + \frac{1}{2} Q''(k_{z1},\theta)(k_z - k_{z1})^2 \ , \text{ near } \ k_z = k_{z1} \\ \\ Q(k_{z2},\theta\ ) + \frac{1}{2} Q''(k_{z2},\theta)(k_z - k_{z2})^2 , \text{ near } \ k_z = k_{z2} \end{cases} \tag{5.9}$$

Then putting $k_z - k_{zi} = \tau$, (5.7) becomes asymptotically

$$E_z(r,\theta) \simeq - \frac{\omega\mu_o\ F(k_{z1})}{4\pi\sqrt{2\pi r \sin\theta}}\ e^{irQ(k_{z1},\theta) + i\frac{\pi}{4}} \int_{-\varepsilon}^{\varepsilon} e^{\frac{ir}{2} Q''(k_{zi},\theta)\tau^2}\ d\tau$$

$$- \frac{\omega\mu_o\ F(k_{2z})}{4\pi\sqrt{2\pi r \sin\theta}}\ e^{irQ(k_{z2},\theta) + i\frac{\pi}{4}} \int_{-\varepsilon}^{\varepsilon} e^{\frac{ir}{2} Q(k_{z2},\theta)\tau^2}\ d\tau + O(\tfrac{1}{r})$$

where ε is a small positive quantity. $Q''(k_z,\theta)$ is given by

$$Q''(k_z,\theta) = -\xi'' \sin\theta \tag{5.10}$$

where $\xi'' < 0$ for $k_z = k_{z1}$ and $\xi'' > 0$ for $k_z = k_{z2}$. Hence, with the substitution $\frac{1}{2} rQ''(k_{z1},\theta)\tau^2 = u^2$ and knowing that $\int_{-\infty}^{\infty} e^{iu^2}\ du = \sqrt{i\pi}$

$$\int_{-\varepsilon}^{\varepsilon} e^{irQ''(k_{z1},\theta)\tau^2}\ d\tau \simeq \left\{\frac{2\pi}{r\left|Q''(k_z,\theta)\right|}\right\}^{1/2} e^{i\pi/4}$$

Similarly,

$$\int_{-\varepsilon}^{\varepsilon} e^{irQ''(k_{z2},\theta)\tau^2} \simeq \left\{\frac{2\pi}{r\left|Q''(k_z,\theta)\right|}\right\}^{1/2} e^{-i\frac{\pi}{4}}$$

Thus we obtain

$$E_z(r,\theta) \simeq -\frac{\omega\mu_o}{4\pi r} \frac{F(k_{z1})}{[\sin\theta|Q''(k_{z1},\theta)|]^{1/2}} e^{irQ(k_{z1},\theta)+\frac{i\pi}{2}}$$

$$+ \frac{F(k_{z2})}{[\sin\theta|Q''(k_{z2},\theta)|]^{1/2}} e^{irQ(k_{z2},\theta)} \quad , \quad 0 < \theta < \theta_o \qquad (5.11)$$

From the foregoing expression for $E_z(r,\theta)$ we see that the fields fall as $1/r$. Since the phase of the two waves in (5.11) are $(-\omega t - \rho\xi(k_{zi})e_\rho + k_{zi}z\, e_z)$, their phase velocities are given by

$$\underline{V}_{pi} = \frac{\omega}{(\xi^2(k_{zi}) + k_{zi}^2)^{1/2}} \qquad (5.12)$$

and it makes an angle ψ with $\underline{B}_o$ where

$$\psi = -\tan^{-1}\left(\frac{\xi'(k_{zi})}{k_{zi}}\right) \quad , \quad i = 1,2 \qquad (5.13)$$

Using equations (5.12) and (5.13) the phase velocity plot as given in Figure 3.2 can be obtained. It can be shown that $V_{p1} > V_{p2}$ and therefore we call the waves given by the first and second term in (5.11) the fast and the slow wave, respectively.

The net field inside the cone will be the interference of the two waves. The structure of the interference pattern will depend upon the relative amplitudes of the two waves.

5.1.2 Field near the Cone

As one approaches the conical surface $\theta = \theta_o$ the two stationary points coalesce and then $Q'' = 0$. The stationary point becomes

second order. Then the expression for $E_z(r,\theta)$ given by (5.8) must be improved. In order to obtain a valid asymptotic representation of the field near the cone, the term $(k_z - k_{zi})^3$ in the Taylor expansion of $Q(k_z,\theta)$ must be included. We therefore expand $Q(k_z,\theta)$ in a double Taylor series and keep terms up to the third order in $(k_z - k_{zi})$ and first order in $|\theta - \theta_o|$. Thus we have

$$Q(k_z,\theta) \simeq A + B\,\tilde{\theta} - \frac{1}{\sin\theta_o}\,\tau\tilde{\theta} - \frac{1}{3!}\,\xi'''(k_{zo})\sin\theta_o\,\tau^3 \qquad (5.14)$$

where $A = Q(k_{zo},\theta_o)$, $B = \frac{d}{d\theta}\,Q(k_{zo},\theta)\Big|_{\theta=\theta_o}$ and $\tilde{\theta} = (\theta - \theta_o)$ and $\tau = (k_z - k_{zo})$.

Combining (5.7) and (5.14) we obtain

$$E_z(r,\theta) \simeq -\frac{\omega\mu_o}{4\pi}\, e^{i[r(A+B\tilde{\theta})+\frac{\pi}{4}]}\, F(k_{zo}) \int_{-\varepsilon}^{\varepsilon} d\tau$$

$$\times \quad e^{-ir[\frac{1}{3!}\,\xi'''(k_{zo})\sin\theta_o\tau^3 + \frac{1}{\sin\theta_o}\,\tilde{\tau}\,\tilde{\theta}]}$$

Defining a new variable t by $t^3 = \frac{1}{2}\,r\,\xi'''(k_{zo})\sin\theta_o\,\tau^3$ we find for the integral (I) in the foregoing expression for $E_z(r,\theta)$

$$I \sim \left[\frac{2}{r\,\xi'''(k_{zo})\sin\theta_o}\right]^{1/3} \int_{-\infty}^{\infty} dt\; e^{-i[\frac{t^3}{3} + \theta\left(\frac{2r^2}{\xi'''(k_{zo})\sin^4\theta_o}\right)^{1/3} t]}$$

The integral in the above expression is the Airy function $Ai(X)$ where

$$X = \tilde{\theta} \left\{ \frac{2r^2}{\xi'''(k_{zo}) \sin^4 \theta_o} \right\}^{1/3} \tag{5.16}$$

Thus we obtain

$$E_z(r,\theta) \simeq - \frac{\omega \mu_o}{(r \sin \theta_o)^{5/6}} \left\{ \frac{1}{\sqrt{2}\, \xi'''(k_{zo})} \right\}^{1/3} \frac{Ai(X)}{\sqrt{\pi}}\, e^{ir(A + B\theta) + \frac{i\pi}{4}} \tag{5.17}$$

The Airy function $Ai(X)$ is oscillatory for $X < 0$ and exponentially decaying for $X > 0$ as shown in Figure 5.2. Thus the field is oscillatory with decreasing amplitude inside the cone ($\tilde{\theta} < 0$) and exponentially decreasing outside the cone ($\tilde{\theta} > 0$). From equation (5.16) the structure of the pattern near the cone surface can be predicted. The spacing $\Delta\theta$

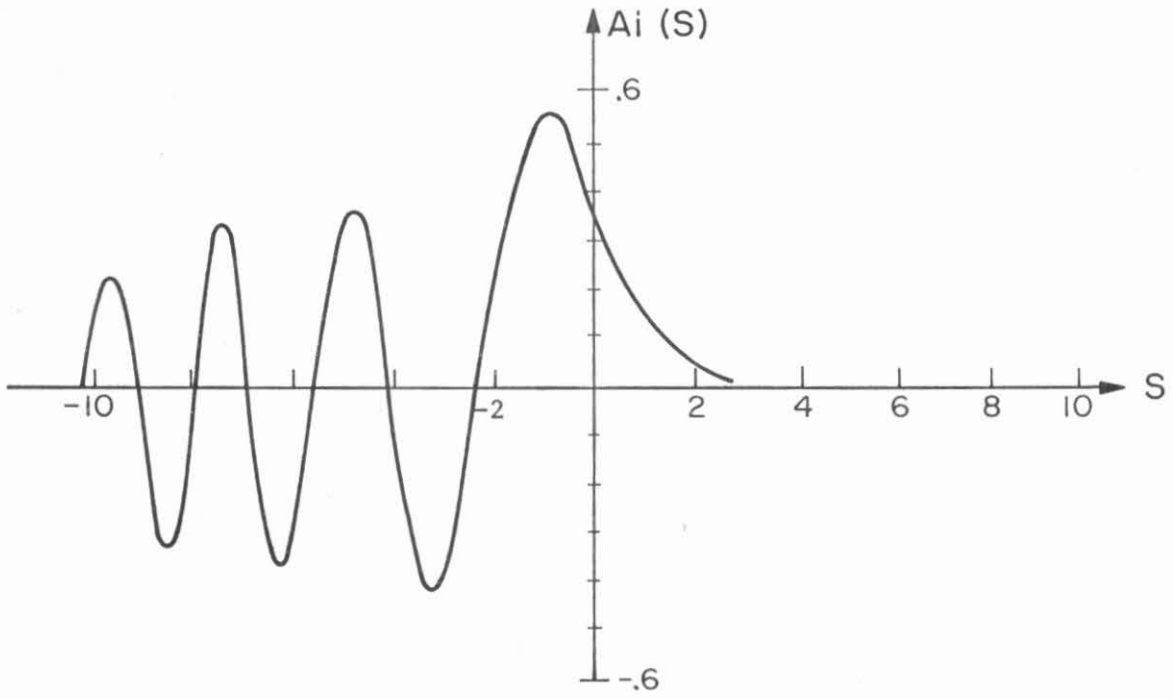

Figure 5.2 Airy function.

between two adjacent maxima or minima of the field pattern near the cone will be given by

$$\Delta\theta = \Delta S \left\{ \frac{\xi'''(k_{zo})\sin^4\theta_o}{2r^2} \right\}^{1/3} \tag{5.18}$$

where ΔS is the spacing between two adjacent maxima or minima of $Ai(S)$. It is clear that $\Delta\theta \sim r^{-2/3}$. In the electrostatic approximation it can be shown that $\epsilon'''(k_{zo}) \propto V_s^2$ and therefore $\Delta\theta \sim V_s^{2/3}$. Since $Ai(X)$ has the first maximum at $X = -1$, the first maximum in the field pattern will occur when

$$\tilde{\theta} = -\left\{ \frac{\xi'''(k_{zo})\sin^4\theta_o}{2r^2} \right\}^{1/3}$$

The field on the cone surface $\tilde{\theta} = 0$ falls as $r^{-5/6}$.

Outside the cone there are no real saddle points. In general, the saddle points will be complex; thus the fields will be evanescent.

It is worth mentioning here that this problem has an analog in fluid mechanics. The water waves generated by thin ships [19] have characteristics like the waves described here.

5.2 Case $\omega > \omega_p$

In the collisionless fluid model of the plasma for $\omega > \omega_p$, ξ is real for $0 < k_z < k_o$ and $\frac{\omega}{V_s}\sqrt{1 - (\omega_p^2/\omega^2)} < k_z < \frac{\omega}{V_s}$. Therefore equation (5.6) will give real stationary points only for these ranges of k_z. Only these real stationary points contribute significantly to the far field. As we will see, the stationary point $\frac{\omega}{V_s}\sqrt{1 - (\omega_p^2/\omega^2)}$ will give a propagating wave in the direction $\theta = 0$.

At this point $K_{||} = 0$ and then the large argument approximation for the Hankel function is no longer valid. Moreover, when $\theta = 0$, $\rho = 0$. Therefore, the integral in equation (5.3) gives good approximation for $E_z(r,\theta)$ only for values of $\theta > 0$.

The choice of value n is made on the basis of the discussion in Section 4.3. We choose $n = 1$ for $0 < k_z < k_o$ and $n = 2$ for $\frac{\omega}{V_s}\sqrt{1 - (\omega_p^2/\omega^2} < k_z < \frac{\omega}{V_s}$. The stationary points are found by plotting θ against k_z according to equation (5.6). Figure 5.3 gives a plot for the stationary points for $\frac{c}{V_s} = 400$ and $\omega_p/\omega = 1/\sqrt{2}$.

Some of the striking features of Figure 5.3 are the following. It clearly shows that there are two modes of propagation. In one of the modes for which the stationary points lie in the range $0 < k_z < k_o$ the waves propagate for all values of θ . This is the mode of radiation one finds in a cold uniaxial plasma. The characteristics of this mode of radiation are very much like radiation from a dipole antenna in free space. Henceforth we call this mode the "electromagnetic mode" and fields in this mode are designated by a subscript e ; for example, E_{ze} .

The other mode, for which the stationary points lie in the range $\frac{\omega}{V_s}\sqrt{1 - (\omega_p^2/\omega^2)} < k_z < \frac{\omega}{V_s}$ is a hot plasma effect. We call this mode the "hot plasma mode". The waves in this mode propagate only within a cone whose axis is along the z-axis and whose cone angle is θ_o . Values of θ_o for several values of ω_p/ω are given in the following table.

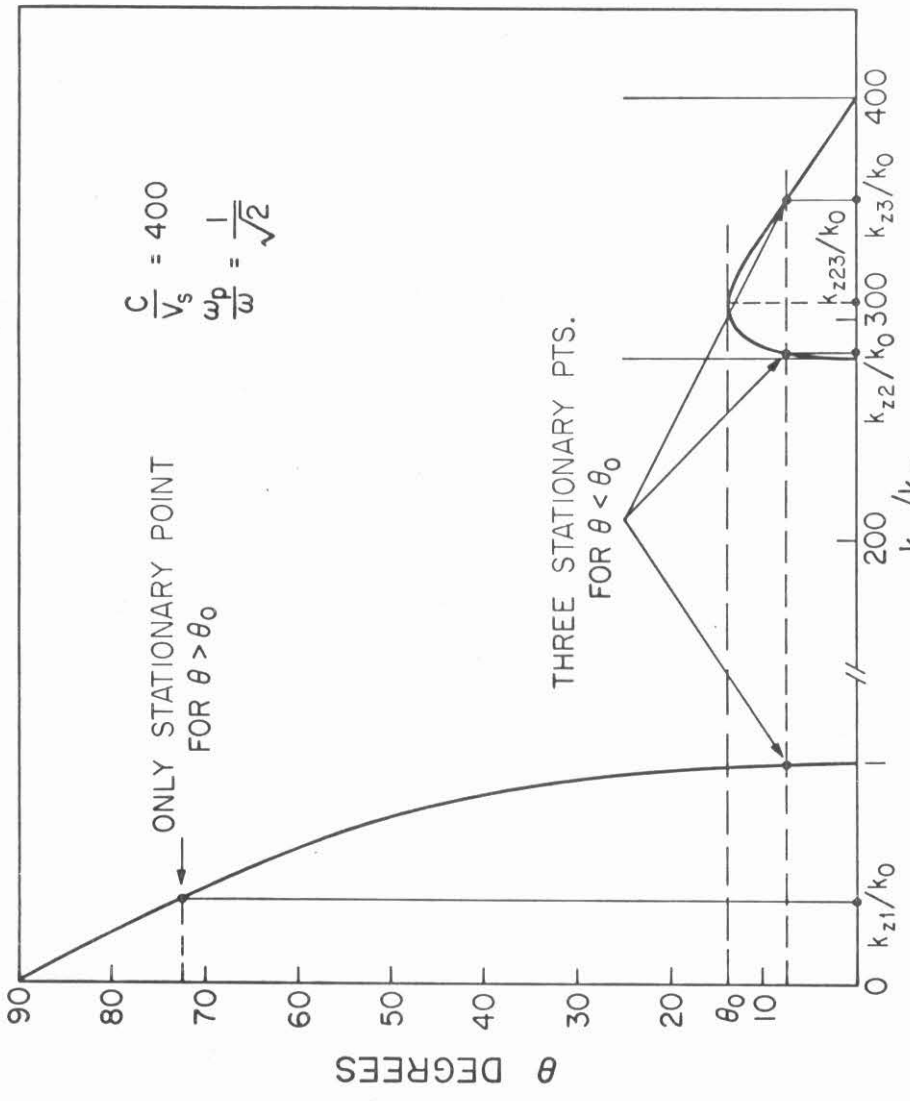

Figure 5.3 Stationary point plot for $\omega > \omega_p$

ω_p/ω	15/16	$1/\sqrt{2}$	1/2	1/5
θ	41.5^o	13^o	5.5^o	$.8^o$

It is seen from this table that the radiation in the hot plasma mode is confined in a very narrow conical region centered along the magnetic field $\underline{B}_o$. The fields in this mode are designated by a subscript p , for example, E_{zp} .

Now, knowing the location of the stationary points, the fields are easily evaluated by the method of stationary phase as outlined in the previous section. The field in the electromagnetic mode is given by

$$E_{ze}(r,\theta) \simeq \frac{\omega\mu_o}{4\pi r} \frac{F(k_{z1})}{[\sin\theta |Q''(k_{z1},\theta)|]^{1/2}} e^{irQ(k_{z1},\theta) - \frac{i\pi}{2}} \qquad (5.19)$$

where $Q(k_{z1},\theta) = \xi(k_{z1})\sin\theta + k_{z1}\cos\theta$.

By constructing a polar plot for the phase and group velocities for the wave in (5.19) we can obtain the same plot as given in Figure 3.3. The phase velocity $\underline{V}_p$ lies in the range $c < V_p < \frac{c}{\sqrt{[1 - (\omega_p^2/\omega^2)]}}$ The field given by (5.19) falls as $1/r$. In the case $V_s/c << 1$, it gives the field of a short electric dipole antenna in a cold uniaxial plasma.

In the hot plasma mode the structure of the field will be very much like the field for $\omega < \omega_p$ (Section 5.2). There will be two propagating waves for $\theta < \theta_o$. Near the cone ($\theta \simeq \theta_o$) the field can be represented by Airy function. Outside the cone the field will be

evanescent. Thus E_{zp}, the z component of the electric field in the hot plasma mode, can be written

$$E_{zp}(r,\theta) \simeq -\frac{\omega\mu_o}{4\pi r} \frac{F(k_{z2})}{[\sin\theta|Q''(k_{z2},\theta)|]^{1/2}} e^{irQ(k_{z2},\theta)+\frac{i\pi}{2}}$$

$$+ \frac{F(k_{z3})}{[\sin\theta|Q''(k_{z3},\theta)|]^{1/2}} e^{irQ(k_{z3},\theta)}, \quad 0 < \theta < \theta_o \qquad (5.20)$$

and

$$E_{zp}(r,\theta) \simeq -\frac{\omega\mu_o}{(\xi \sin\theta_o)^{5/6}} (\sqrt{2}\ \xi'''(k_{z23}))^{-1/3}$$

$$\tilde{Ai}\left(\tilde{\theta}\left\{\frac{2r^2}{\xi'''(k_{z23})\sin^4\theta_o}\right\}^{1/3}\right) e^{ir(A+B\theta)+\frac{i\pi}{4}}, \quad \theta \simeq \theta_o \qquad (5.21)$$

where k_{z2}, k_{z3} and k_{z23} are defined in Figure 4.3, and $A = Q(k_{z23},\theta_o)$, $B = \frac{d}{d\theta} Q(k_{z23},\theta)\Big|_{\theta=\theta_o}$.

The phase and the group velocity plot in Figure 3.4 corresponds to the two waves given by equation (5.20).

It is important to note that the entire discussion in this chapter is based on collisionless fluid model of the plasma. The Landau and the collisional damping are not considered. In the presence of any damping the slow wave for $\omega < \omega_p$ and the waves in the hot plasma mode

for $\omega > \omega_p$ will damp away in the far zone. Since the stationary points are determined by the slope $d\xi/dk_z$, the stationary point plots in Figures 5.2 and 5.3 which are for the fluid model of the plasma, can be modified in some respects by considering the kinetic model. But it is expected that the basic characteristics of the plots will remain unchanged.

VI. NEAR FIELDS

The study of the near field of a probe or an antenna in a magneto-plasma is useful from the viewpoint of laboratory diagnostics. Measurements of nearfield pattern can render information about the electron density and temperature[12]. By numerical evaluation of the integrals in 4.15a, b and c the effects of collisional and Landau damping, dipole length, electron thermal velocity and distance from the source on the angular distribution of the near field pattern have been studied in this chapter. This study sheds some light on how to measure some of the plasma parameters in the laboratory. The Landau damping is included in the following calculations by using (2.17) for $K_{||}$ in the expression for ξ in (2.19).

6.1 Case $\omega < \omega_p$.

In Chapter V it was found that the far field consists of two propagating waves, a slow wave and a fast wave, and these waves propagate only within a cone whose cone angle is slightly less than $\sin^{-1} \omega/\omega_p$. The numerical calculation of the near field demonstrates that two waves interfere within this cone and outside of this cone the field falls off rapidly.

(a) Collisional and Landau Damping

Figure 6.1 shows a field pattern of E_z in fluid and kinetic theory models of the plasma. This figure has several interesting features. At small collision frequency this pattern shows no inter-

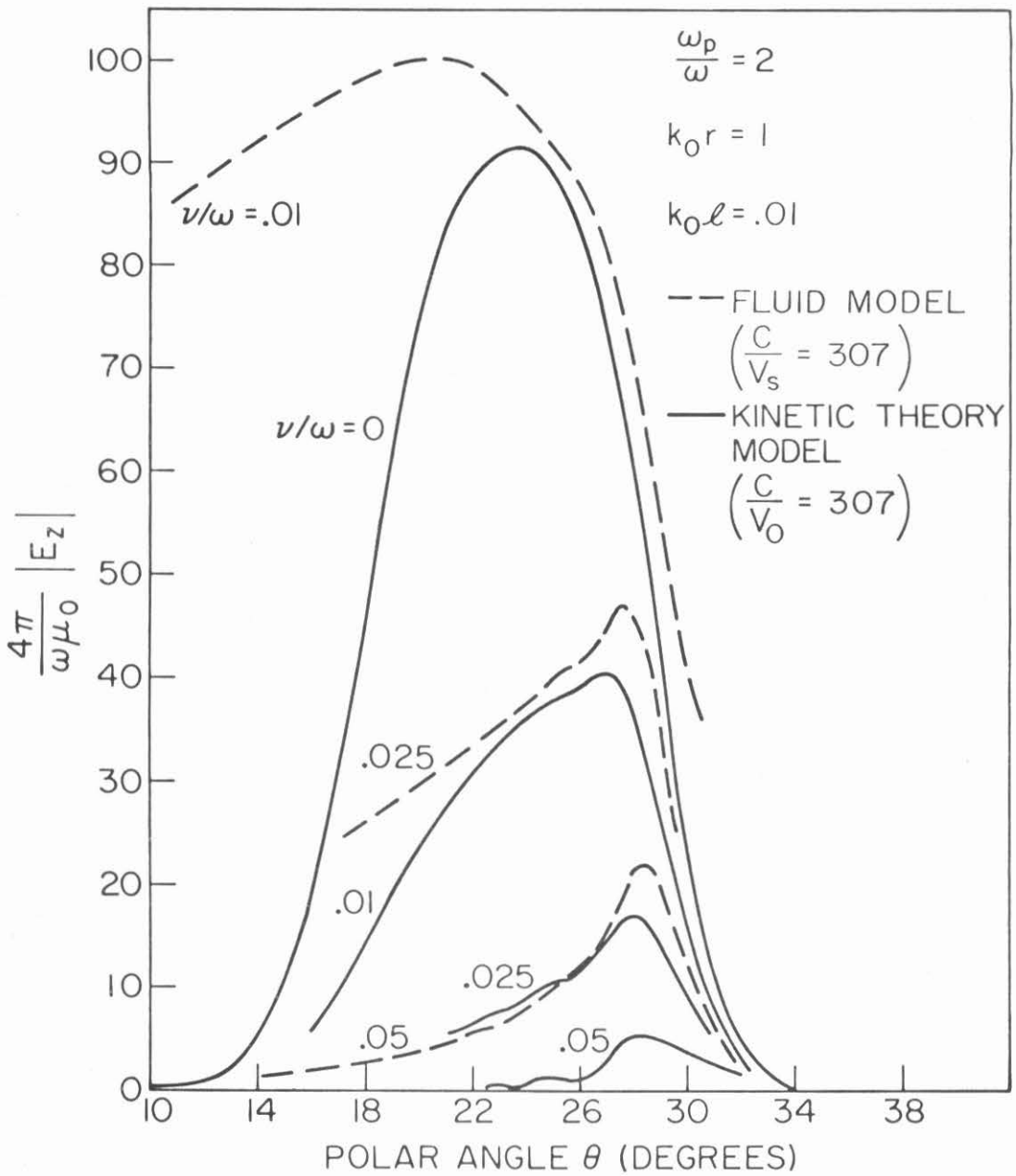

Figure 6.1 Effects of collisional and Landau damping on the interference structure in the angular distribution of the field pattern.

ference. Even the inclusion of Landau damping at small collision frequency shows no interference. Only when the collision frequency is sufficiently large is interference of the two waves in the angular distribution of the field pattern noted. In order that the two waves interfere and give several maxima and minima in the field patterns the amplitudes of the two interfering waves should be comparable. Moreover the slow wave is more susceptible to collision damping than the fast wave. In which case, for the value of parameters shown in Figure 6.1, the dipole excites the slow wave much more than the fast wave. Collisional and Landau damping reduce the amplitude of the slow wave and thus make the amplitude of the two waves comparable at a certain distance from the source.

Furthermore, it can be seen from Figure 6.1 that by increasing the collision frequency the cone angle, where maxima in the field pattern occurs, moves closer to $\sin^{-1} \omega/\omega_p$. The appearance of the slow wave is a hot plasma effect. In the limit where one collision frequency tends to be large, temperature effects become less important and results of cold plasma theory with collisions can be recovered from this treatment.

The field patterns in Figure 6.2 clearly demonstrate the interference phenomenon. These field patterns are for different values of ω/ω_p and $\nu/\omega = .05$. Increasing ω/ω_p increases the cone angle, hence for a given value of r, the cone occurs at larger radial distance ρ. Since $(\xi\rho)$ is the argument of the Hankel function in the integral expressions (4.15), the slow waves are more damped. This gives interference patterns with well defined maxima and minima. But

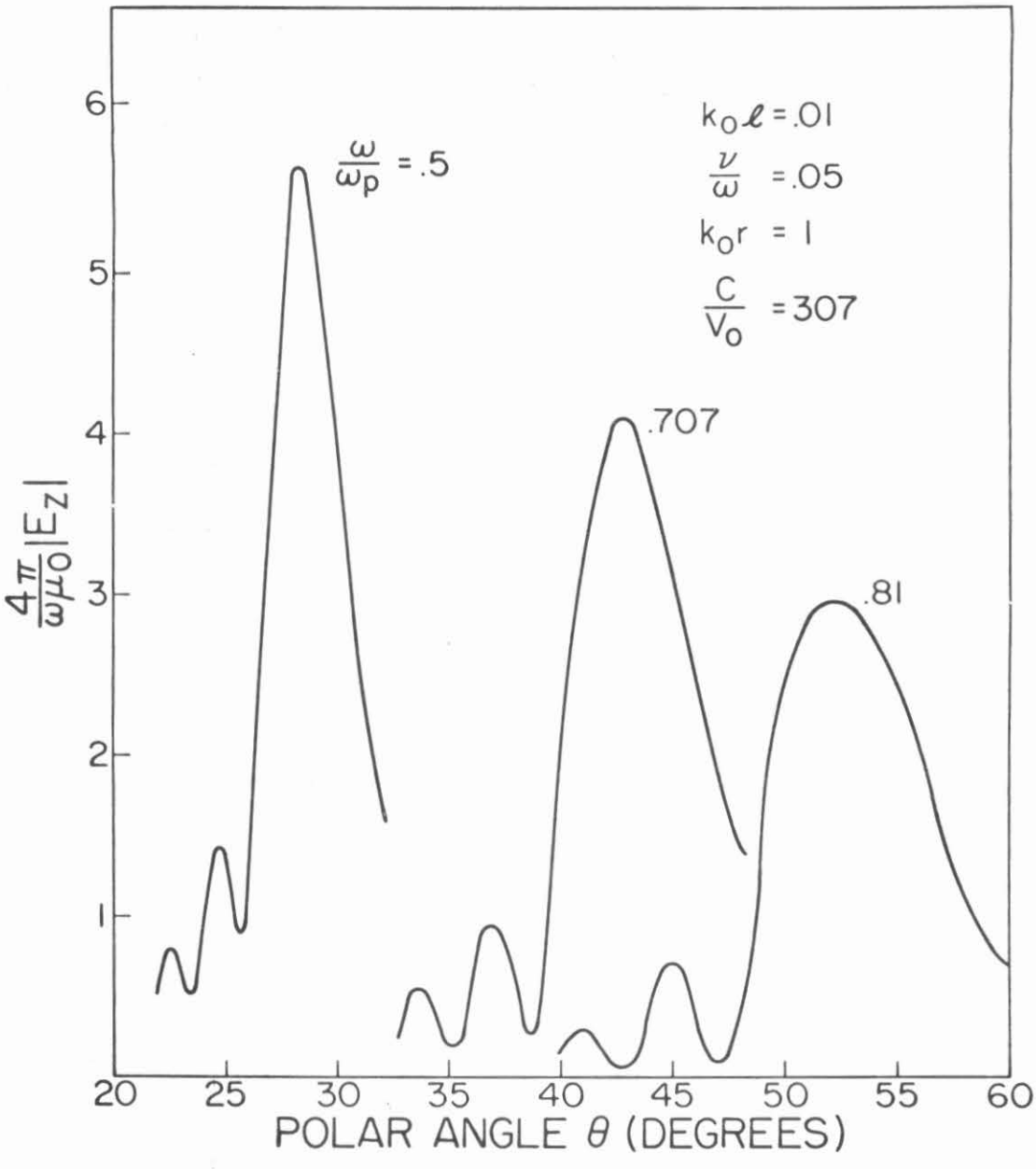

Figure 6.2 Diagram demonstrating well defined maxima and minima in the angular distribution of the field pattern.

it is expected that when ω/ω_p is large enough so that the slow waves are completely damped out the interference structure will disappear. The interference pattern with well defined maxima and minima (at a certain distance r from the source) appears only for certain range of values of ω/ω_p. The stretch of the range depends on the distance r.

The experimental study of the field patterns by Fisher [12] compare qualitatively with these theoretical interference patterns. In this experiment the collision frequency is much smaller than one used for obtaining the field patterns in Figure 6.2. It is expected that the sheath around the probe in this experiments damps the slow wave which propagate inside the cone. Thus it is possible for interference patterns with several maxima and minima to appear with a smaller collision frequency.

(b) Dipole Length:

The length of a dipole in a magnetoplasma can play an important role in determining the field pattern. Angular distributions of the field for several dipole lengths are given in Figure 6.3 for the kinetic theory model of the plasma. For a very short dipole the field pattern shows no interference of the two waves. By increasing one length of the dipole, field patterns with several maxima and minima appear. This has the following simple explanation. When the dipole is very short it is a more effective radiator of the short wavelength waves, which are the slow waves, than of the fast waves. As the dipole becomes longer it radiates more fast waves and beyond a certain length it radiates less and less of slow waves. Hence when

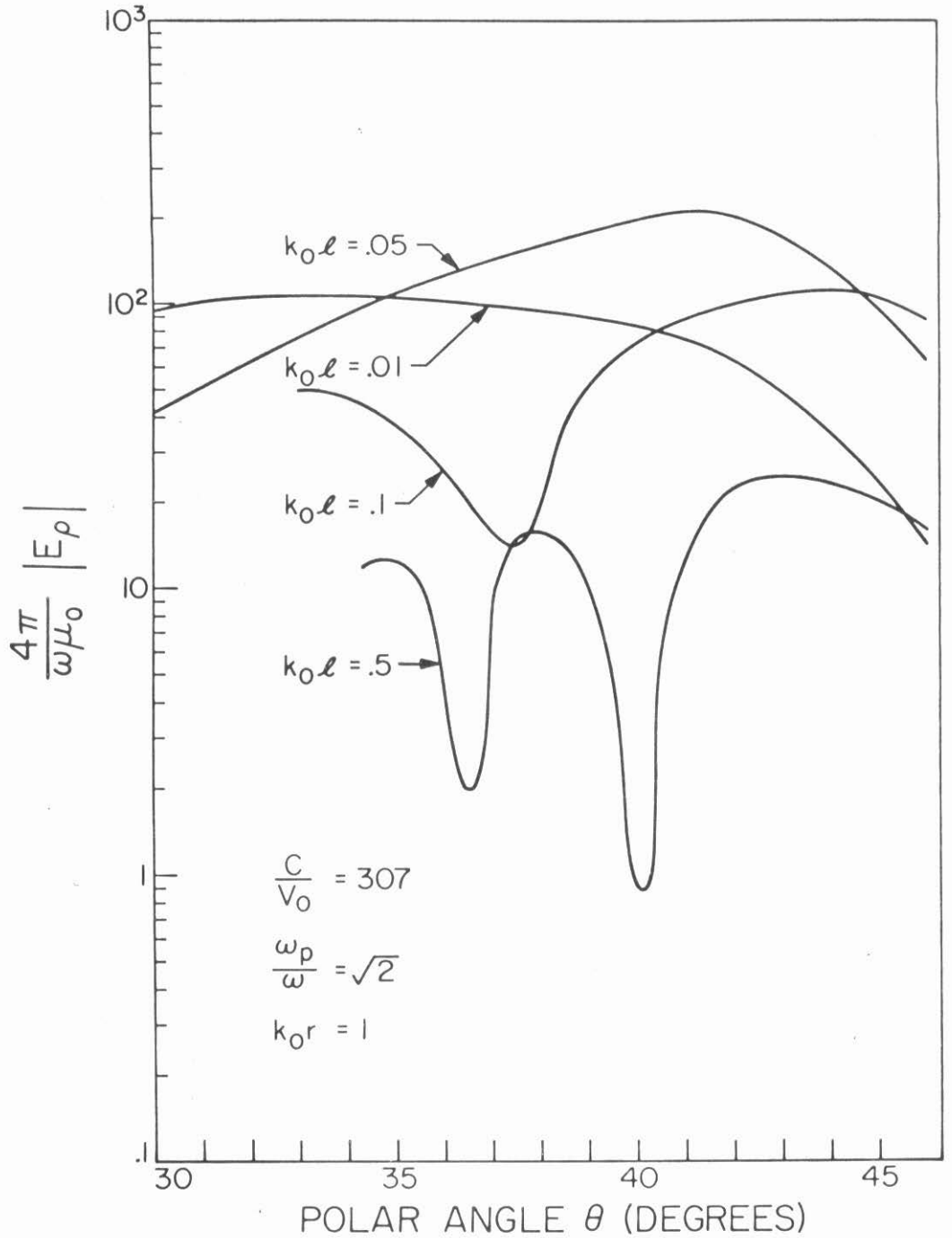

Figure 6.3 Effect of dipole length on the interference structure in the angular distribution of the field pattern.

the dipole becomes long enough so that the amplitudes of the two waves are comparable, they interfere to give several maxima and minima in the field pattern. When the dipole becomes too long the fast wave becomes much larger than the slow wave, and then the interference structure disappears.

(c) Electron Thermal Velocity:

Effect of the electron thermal velocity on the interference of the two waves and the angular distribution of the field pattern is shown in Figure 6.4. It can be seen from this figure that the height of the cone increases almost linearly with c/V_o.

Also the cone angle approaches $\sin^{-1} \omega/\omega_p$ as V_o gets smaller. In the limit V_o tends to zero; the fields become infinite on the conical surface of cone angle $\sin^{-1}(\omega/\omega_p)$. This is the result of linear cold plasma theory. Hot plasma effects make the fields finite at this angle. The spacing $\Delta\theta$ between the two adjacent maxima and minima and the shift in the cone angle from $\sin^{-1}(\omega/\omega_p)$ go as $(c/V_o)^{-2/3}$. The warmer the plasma, the greater the spacing $\Delta\theta$ and shift in the cone angle. These results can be compared with the asymptotic representation of the fields near the cone in the preceding chapter. Near the cone the fields are represented by the Airy function. Studying the argument of the Airy function one can predict the above results.

(d) Distance r from the Origin:

Figure 6.5 gives field patterns for several values of the normalized distance $(k_o r)$. The height of the cone falls approximately as $r^{-2/3}$. The spacing $\Delta\theta$ between the two adjacent maxima or minima

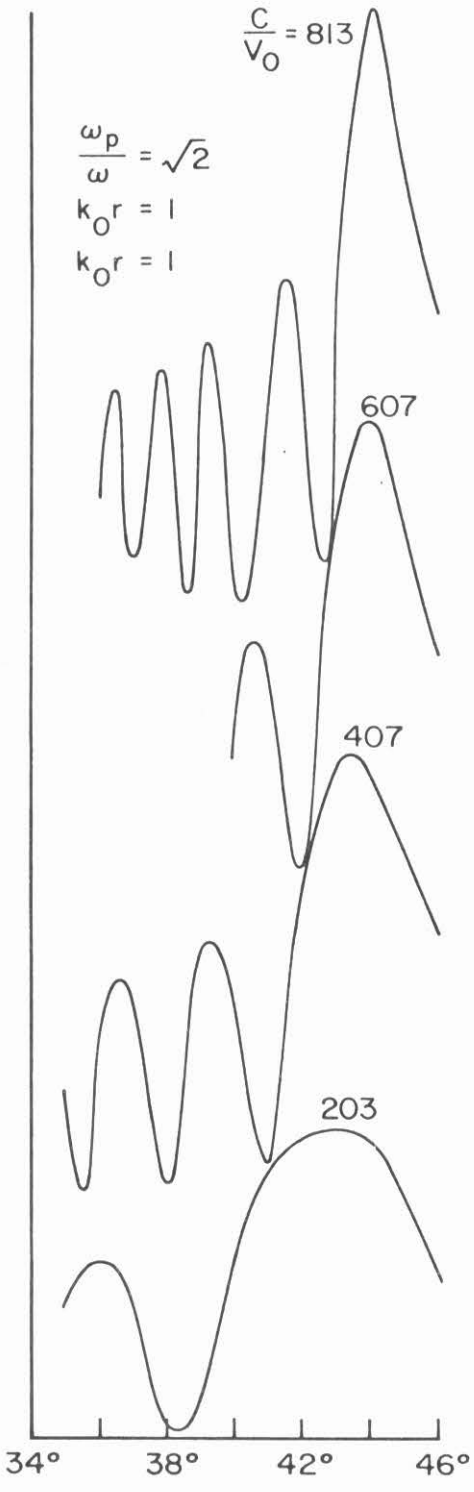

Figure 6.4 Diagram showing increasing cone height and decreasing interference spacing $\Delta\theta$ with decreasing electron thermal speed V_o.

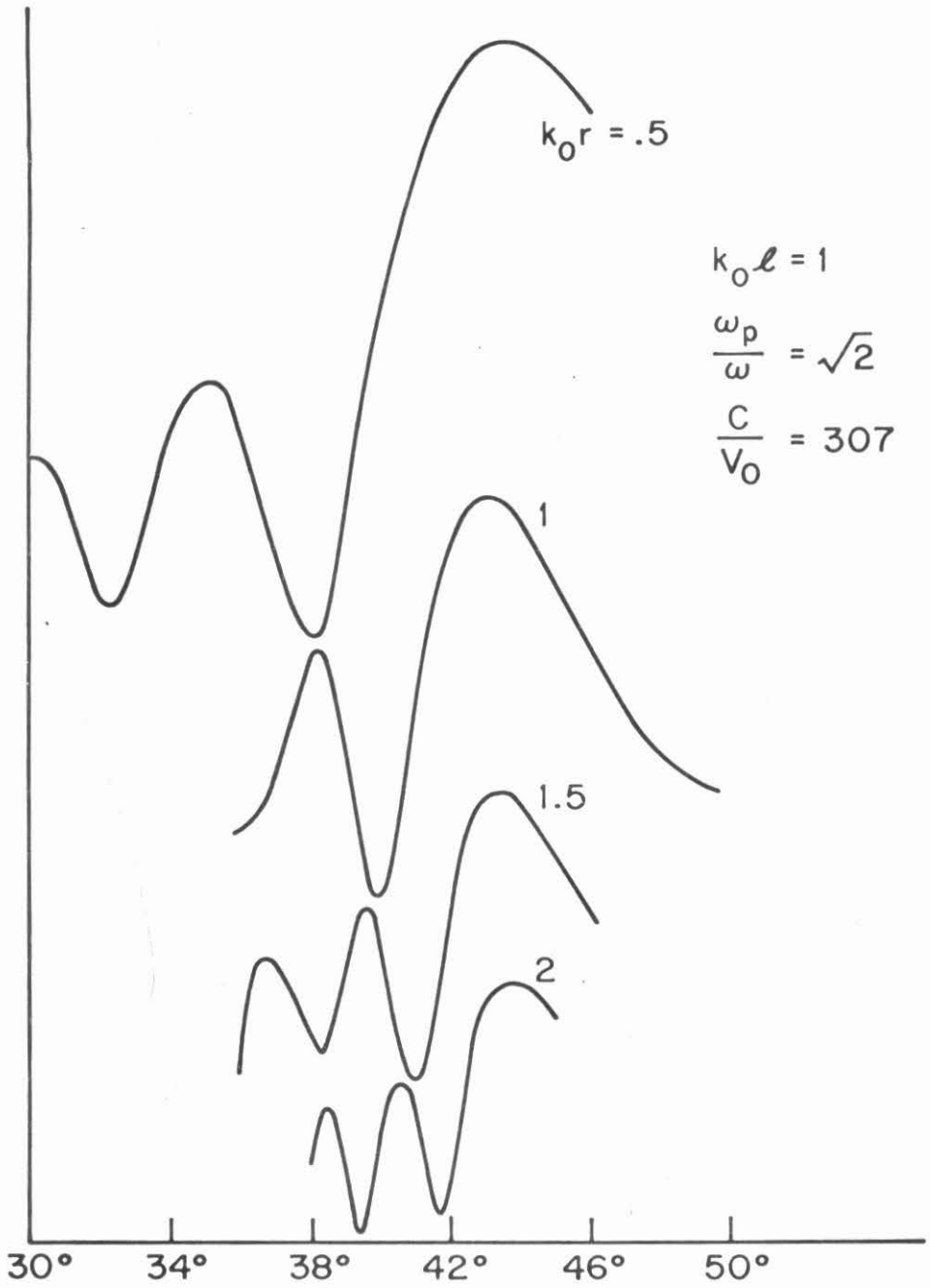

Figure 6.5 Diagram showing decreasing cone height and decreasing interference spacing $\Delta\theta$ with increasing distance from the antenna.

and the shift in the cone angle from $\sin^{-1} \omega/\omega_p$ behave as $(k_o r)^{-2/3}$. This has been verified experimentally by Fisher and Gould [20] . This behavior can also be seen from the asymptotic representation of the field near the cone in Chapter V. This implies that as one moves farther from the antenna he will observe more numbers of oscillations in the angular distribution of the field. Combining the effects of thermal velocity with this, one can see that

$$\Delta\theta \simeq A \left(\frac{\omega r}{V_o}\right)^{-\frac{2}{3}} \tag{6.1}$$

where A will be constant for a given value of ω/ω_p .

6.2 Case $\omega > \omega_p$:

We found in the preceding chapter that for $\omega > \omega_p$ the antenna excites three waves. One of the waves was recognized as the radiation into the electromagnetic mode E_e. The other two waves, which are hot plasma effects were recognized as the radiation into the hot plasma mode E_p .

Figure 6.6 shows a typical field pattern for the electromagnetic mode of radiation. This polar plot resembles the field pattern of a short dipole in free space. The electron thermal velocity has negligible effect on this wave.

A field pattern for E_{zp} is given in Figure 6.7. The shape of this pattern will change with ω/ω_p, the length of the dipole and the electron thermal velocity V_o. But nevertheless it shows an interference of the two waves.

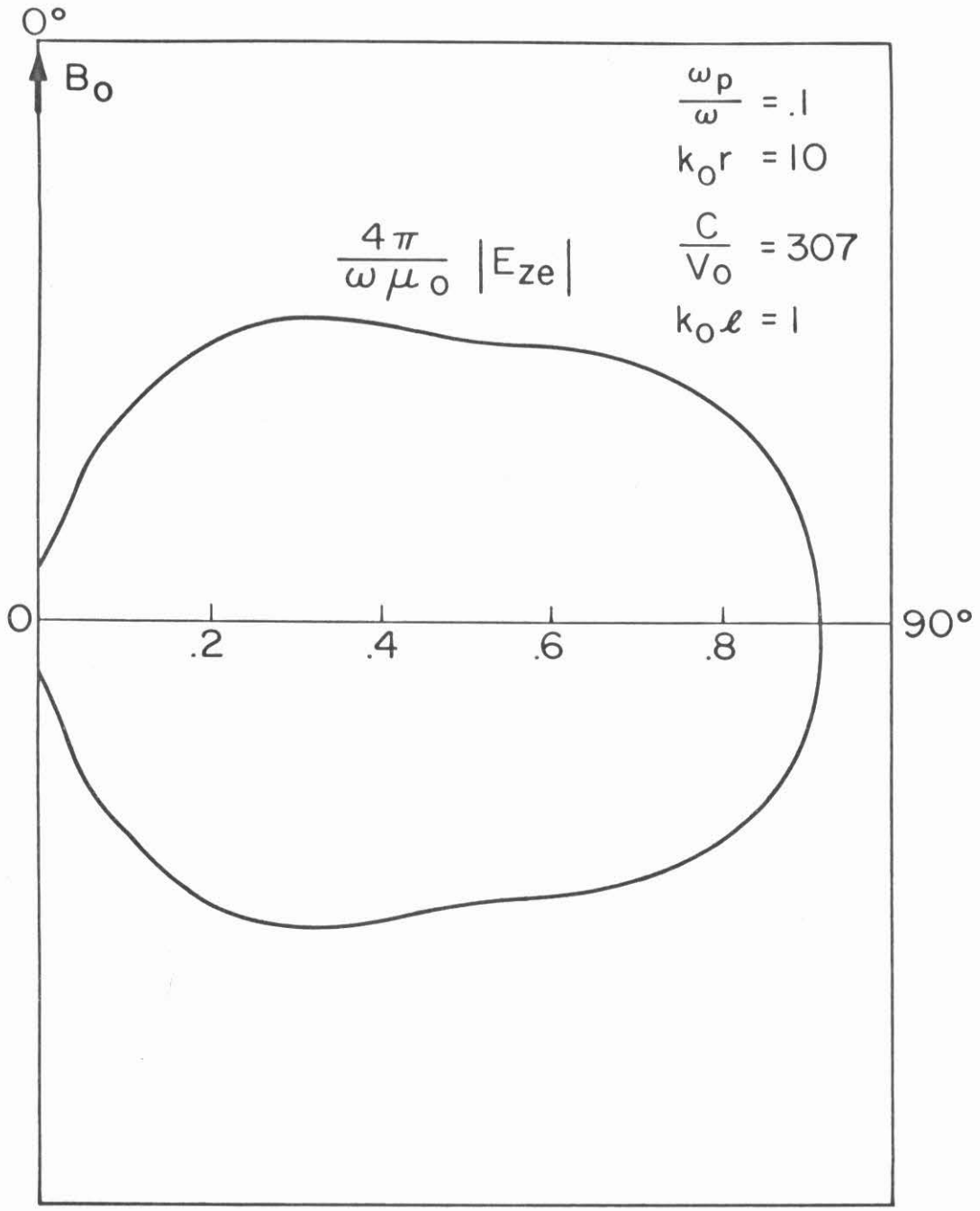

Figure 6.6 Polar plot of the z-component of the electric field in the electromagnetic mode.

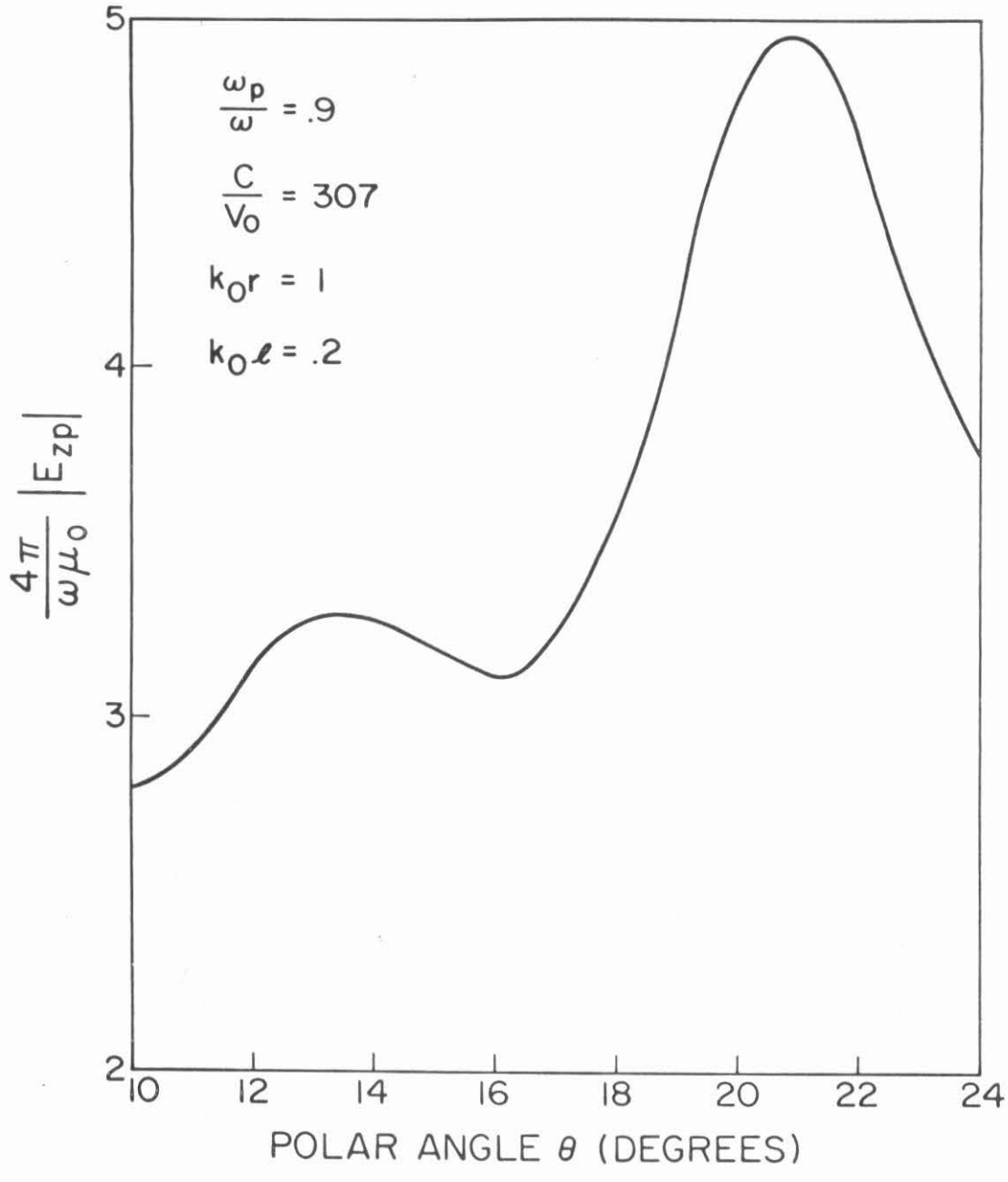

Figure 6.7 Angular distribution of the z-component of the electric field in the hot plasma mode.

When the length of the dipole is such that $k_o \ell \geq 1$ and $\omega >> \omega_p$, E_p becomes negligible compared to E_e, and the dipole becomes primarily a radiator of the electromagnetic waves.

6.3 Diagnostic Techniques:

It was stated at the beginning of this chapter that the study of the near fields may be useful for diagnoising plasma in a magnetic field. Here some experiments are mentioned for measuring the electron density and temperature. Measurement of the cone angle in the angular distribution of the field pattern of a probe in a magnetoplasma can give an estimate of the plasma density. The half cone angle for a cold plasma is given by $\sin^{-1}(\omega/\omega_p)$. The electron temperature shifts this angle to smaller value. Figure 6.8 which is derived from Figure 6.4, gives a plot for the shift against $(\omega r/V_o)^{-2/3}$. This figure also gives the spacing $\Delta\theta$ between first two maxima as function of $(\omega r/V_o)^{-2/3}$. This plot is for $\omega/\omega_p = 1/\ 2$. Similar plots for other values of ω/ω_p can be supplied. A measurement of the spacing between first two maxima or the shift in the cone angle can give an estimate of the electron temperature in terms of V_o. These experiments have been carried out by Fisher and Gould [20].

One must remember that the above considerations are valid only when the magnetostatic field B_o is very large and the plasma density is low such that the cyclotron frequency $\omega_c >> \omega_p$. The source frequency ω should be chosen so that $\omega < \omega_p$ for which the resonance cone in the field pattern appears. The appearance of the resonance cone in the field pattern is advantageous from the view

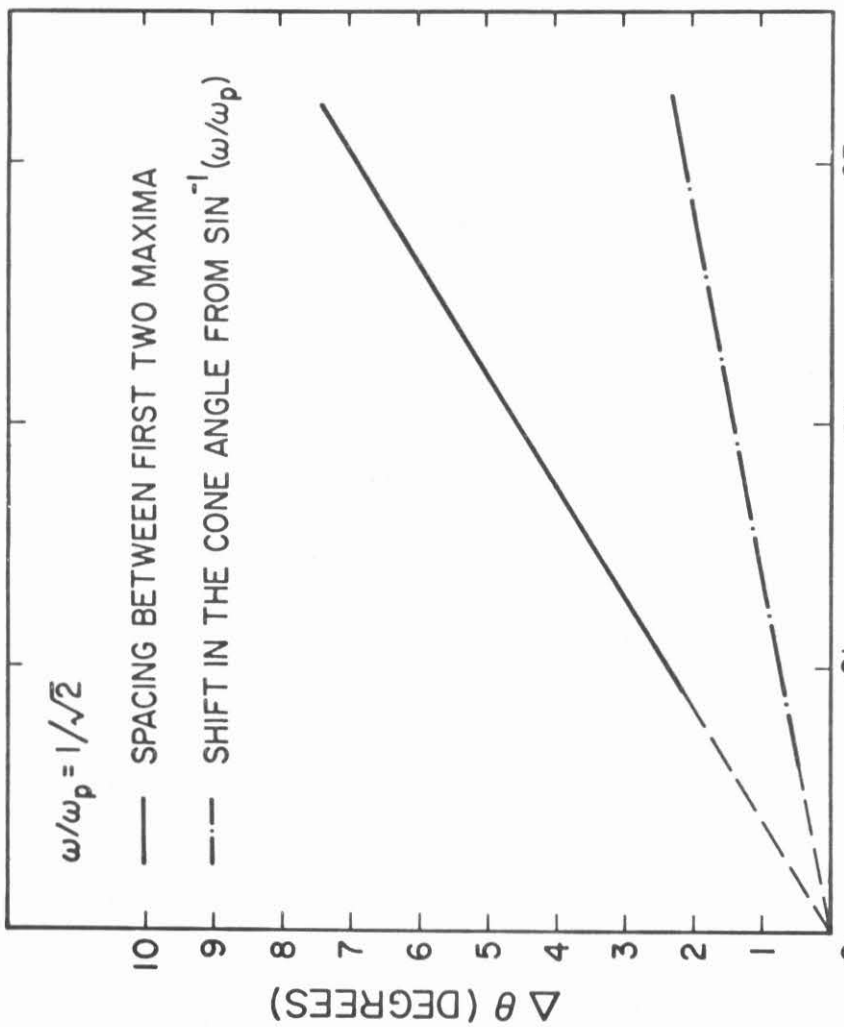

Figure 6.8 Angular interference spacing dependence on $(\omega r/V_o)^{-2/3}$.

point of diagnostic in a small volume of laboratory plasma. In such a situation reflections from the walls do not appear to come back to the probe.

VII. THE INPUT AND THE RADIATION RESISTANCES

In this chapter the input and the radiation resistances of a short dipole antenna oriented along the magnetostatic field are studied. In a lossless plasma the input and the radiation resistances are equal. When the plasma is lossy the input resistance can no longer be called the radiation resistance. The radiated power decreases with the distance from the antenna. In the fluid description of the plasma in absence of collisions the medium is lossless. But in the kinetic description the plasma becomes lossy because of the Landau damping. The effect of the Landau damping on the input resistance and the radiated power is discussed.

7.1 The Input Resistance

The time average input power of the antenna is given by

$$P = -\frac{1}{2}\,\mathrm{Re}\int_V \underline{E}_z(\rho,z)\cdot\underline{J}_s^*(\rho,z)\,dV \tag{7.1}$$

where 'Re' indicates real part. Using Parseval theorem, 7.1 can be written

$$P = -\frac{1}{2}\frac{1}{(2\pi)^3}\,\mathrm{Re}\int_{-\infty}^{\infty}\int_0^{\infty}\int_0^{2\pi}\hat{\underline{E}}_z(\gamma,k_z)\cdot\hat{\underline{J}}_s^*(k_z)\,\gamma\,dk_z\,d\gamma\,d\phi \tag{7.2}$$

$\hat{\underline{E}}_z(\gamma,k_z)$ and $\hat{\underline{J}}_s(k_z)$ are the Fourier transforms of $E_z(\rho,z)$ and $\underline{J}_s(z)$, respectively. Taking the Fourier transforms of (2.18) with respect to the transverse co-odinates we obtain

$$\hat{E}_z(\gamma,k_z) = - i\omega\mu_o \frac{(1-k_z^2/k_o^2)\hat{J}_s(k_z)}{-\gamma^2+K_{||}(k_o^2-k_z^2)} \tag{7.3}$$

The functional form of $\hat{J}_s(k_z)$ depends upon the assumed current distribution.

Substituting (7.3) in (7.2) and performing the integral with respect to ϕ we obtain for the input resistance $(R_{||} = 2P/I_o^2)$

$$R_{||} = + \frac{\omega\mu_o}{2\pi^2} \text{Im} \int_o^\infty dk_z (1-k_z^2/k_o^2)\hat{J}_s^2(k_z) \int_o^\infty \frac{\gamma d\gamma}{\gamma^2-K_{||}(k_o^2-k_z^2)} \tag{7.4}$$

The integral with respect to γ in the foregoing expression for R can be performed to give

$$\int_o^\infty \frac{\gamma d\gamma}{\gamma^2-K_{||}(k_o^2-k_z^2)} = \frac{1}{2} \ell n(P) \Bigg|_{-K_{||}(k_o^2-k_z^2)}^{\infty}$$

The real part of this integral is infinite. But for the imaginary part we have

$$\text{Im} \frac{1}{2} \ell n(P) \Bigg|_{-K_{||}(k_o^2-k_z^2)}^{\infty} = - \frac{1}{2} \tan^{-1}\left(\frac{\text{Im}K_{||}}{R_e K_{||}}\right) - \frac{1}{2} \text{Im}[\ell n (k_z^2-k_o^2)] \tag{7.5}$$

$$\text{Im}\ell n(\lambda^2-k_o^2) = \begin{cases} 0 & k_z > k_o \\ \pm\pi i & k_z < k_o \end{cases}$$

The divergence in the real part of the integral implies that the

reactance of the filamentary antenna is infinite. Similar divergence in the reactance is noted for a filamentary antenna even in the free space. Consideration of finite thickness of the dipole will remove this divergence. Substituting (7.5) into (7.4) the expression for $R_{||}$ becomes

$$R_{||} = \mp \frac{\omega\mu_o}{4\pi} \int_o^{k_o} (1 - \frac{k_z^2}{k_o^2}) \hat{J}_s^2(k_z) dk_z + \frac{\omega\mu_o}{4\pi^2} \int_o^{\infty} (\frac{k_z^2}{k_o^2} - 1) J_s^2(k_z) \tan^{-1}\left(\frac{ImK_{||}}{ReK_{||}}\right) dk_z \tag{7.6}$$

This expression for the input resistance must reduce to that of the free space case when $K_{||} = 1$. In that case the second term in the foregoing expression is zero. Only the first term is non-zero. Hence we must choose the positive sign. Now the input resistance, (hence the total input power) given by foregoing expression is always positive. This can be shown as following. We break the second integral in (7.6) in two parts from zero to k_o and from k_o to ∞, and then combine the first part to the first term (+sign) in (7.6). Since $0 < \tan^{-1}(ImK_{||}/ReK_{||}) < \pi$, this combination will be positive. Also, $(k_z^2/k_o^2 - 1) \geq 0$ for $k_o \leq k_z \leq \infty$, the second part of the second term will always be positive. Hence the entire expression for $R_{||}$ will always be positive. Rewriting this expression we have

$$R_{||} = \frac{\omega\mu_o}{4\pi}\int_o^{k_o}(1-\frac{k_z^2}{k_o^2})(1-\frac{1}{\pi}\tan^{-1}(\frac{ImK_{||}}{ReK_{||}}))\hat{J}_s^2(k_z)dk_z$$

$$+\frac{\omega\mu_o}{4\pi^2}\int_{k_o}^{\infty}(\frac{k_z^2}{k_o^2}-1)\tan^{-1}(\frac{ImK_{||}}{ReK_{||}})\hat{J}_s^2(k_z)dk_z \qquad (7.7)$$

The expression in 7.7 is a general expression for the input resistance. In a lossless plasma this also gives the total radiation resistance. A number of special cases can be derived from it.

7.2 Case $\omega < \omega_p$

In this case one obtains infinite [3] input resistance for a point dipole antenna in a cold plasma. Here we show that the input resistance is always finite for non-zero electron thermal velocity V_s.

7.2.1 Fluid Model of the Plasma

For the fluid model of the plasma $K_{||}$ is given by 2.11. When $\nu=0$, $K_{||} < 0$ for $0 < k_z < \omega/V_s$ and $K_{||} > 0$ otherwise. Hence $\tan^{-1}(ImK_{||}/ReK_{||}) = \pi$ for $0 < k_z < \omega/V_s$ and zero otherwise. Thus we obtain from 7.7

$$R_{||} = \frac{\omega\mu_o}{4\pi}\int_{k_o}^{\omega/V_s}(\frac{k_z^2}{k_o^2}-1)\hat{J}_s^2(k_z)dk_z \qquad (7.8)$$

So far no assumption has been made about $J_s(z)$. To make some quantitative study of $R_{||}$ we assume a triangular current distribution

Given by

$$J_s(z) = \left(1 - \frac{|z|}{\ell}\right); \quad |z| \leq \ell$$

Therefore, $$\hat{J}_s(k_z) = \ell \left(\frac{\sin (k_z \ell/2)}{k_z \ell/2}\right)^2 \tag{7.9}$$

Substituting 7.9 in 7.8 and making a change of variable $k_z = (\omega/V_s)x$ we obtain

$$R_{||} = \frac{1}{4\pi}\sqrt{\frac{\mu_o}{\varepsilon_o}}\, F(k_o\ell), \tag{7.10}$$

where $$F(k_o\ell) = \left(\frac{c}{V_s}\right)^3 (k_o\ell)^2 \int_{V_s/c}^{1} (x^2 - V_s^2/c^2)\left(\frac{\sin\left(\frac{x\omega\ell}{2V_s}\right)}{\frac{x\omega\ell}{2V_s}}\right)^4 dx \tag{7.11}$$

When the length ℓ is such that $\omega\ell/2V_s << 1$

$$F(k_o\ell) = \left(\frac{c}{V_s}\right)^3 (k_o\ell)^2 \int_{V_s/c}^{1} (x^2 - V_s^2/c^2)\, dx$$

We have for $V_s/c << 1$,

$$R_{||} \simeq \frac{1}{4\pi}\sqrt{\frac{\mu_o}{\varepsilon_o}}\, (k_o\ell)^2 \left(\frac{c}{V_s}\right)^3 \tag{7.12}$$

It is interesting to note from 7.12 that when the length of the dipole is much less than the Debye length ($\lambda_d \simeq V_x/\omega_p$), the input resistance behaves as ℓ^2. In the limit ℓ tends to zero $R_{||}$ goes to zero as ℓ^2.

Figure 7.1 Displays the functional dependence of $R_{||}$ (Formula 7.10) on the length of the dipole for several values of c/V_s. The curves in this figure are obtained by evaluating the integral in 7.11 numerically. These

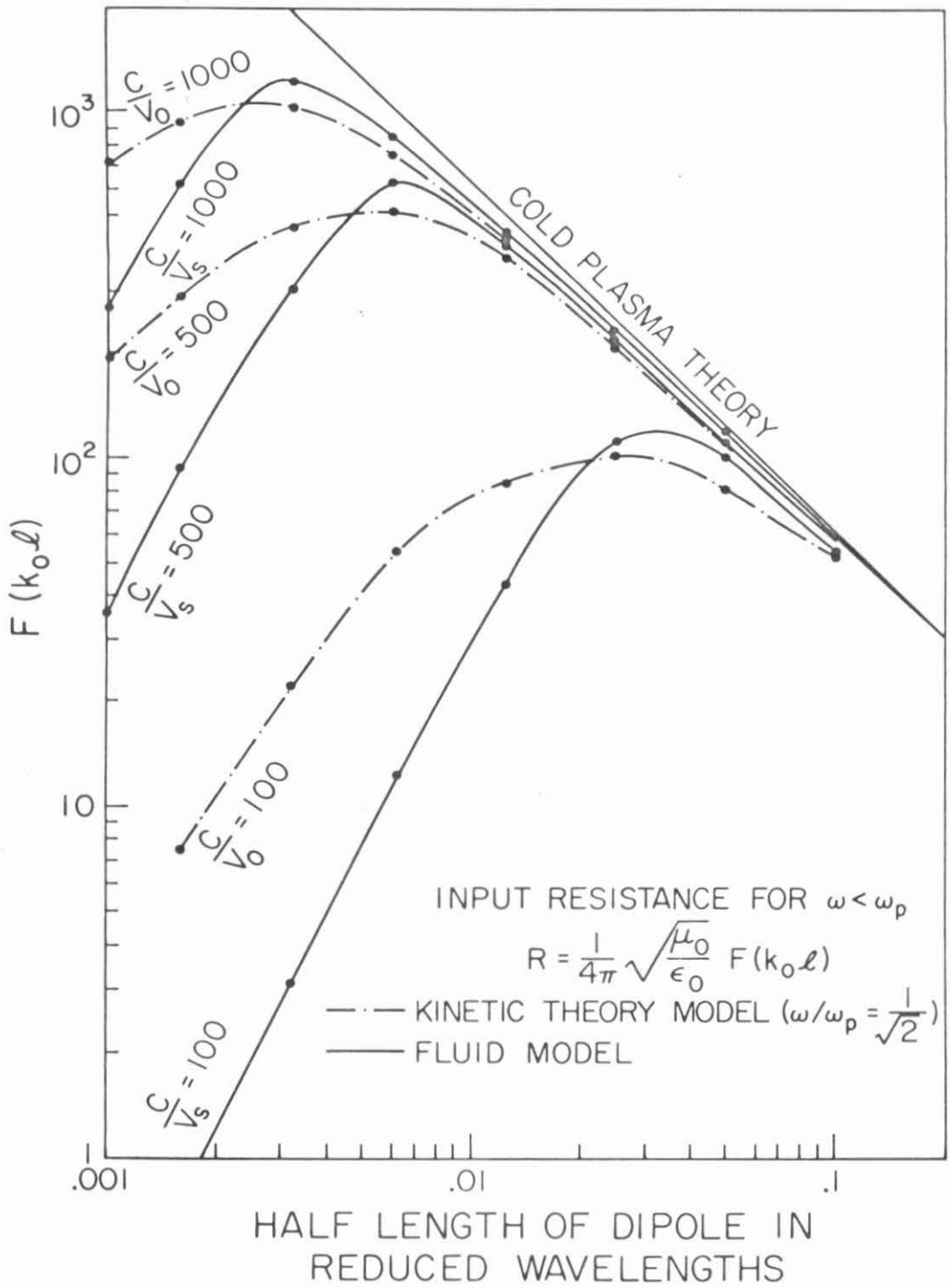

Figure 7.1 Functional dependence of the input resistance on dipole length for $\omega < \omega_p$.

curves show that only when the length of the dipole is much larger than the Debye length such that $\ell >> V_s/\omega$, $R_{||}$ behaves as ℓ^{-1}. The cold plasma theory [17,22] gives that $R_{||}$ behaves as ℓ^{-1} for all lengths and thus when ℓ goes to zero $R_{||}$ becomes infinite.

This behavior of the input resistance can be explained on the basis of the results of Chapter V. We found there that for $\omega < \omega_p$ the antenna excites two waves, a fast wave and a slow wave. The slow waves are very short wavelength waves ($\approx\lambda_d$), while the fast waves have wavelengths ranging from few Debye lengths to the free space wavelength. But for the fast wave most of the power is concentrated in the short wavelength fields near the cone surface. When the antenna length is such that $\ell << \lambda_d$ it radiates short wavelengths very effectively and the input resistance increases as ℓ^2. But when $\ell >> \lambda_d$, the effectiveness of the antenna in radiating the short wavelength waves decreases because of the dephasing of the radiation from its different elements, and then the input resistance falls. For the current distribution assumed it falls as ℓ^{-1}.

7.2.2 Kinetic Theory Model of the Plasma

In the kinetic theory model of the plasma, $K_{||}$ is given by (2.17) and it is rewritten here

$$K_{||} = 1 - \frac{\omega_p^2}{\omega^2} Z'(\omega/k_z V_o)$$

The imaginary part of $K_{||}$ is given by [12]

$$\mathrm{Im}(K_{||}) = 2\sqrt{\pi}\ \frac{\omega_p^2}{\omega}\left(\frac{\omega}{k_z V_o}\right)^3 e^{-\left(\frac{\omega}{k_z V_o}\right)^2} \tag{7.13}$$

For very small k_z ($k_z < k_o$) $\mathrm{Im}(K_{||})$ is almost zero when (c/V_o) is fairly large. $\mathrm{Re}Z'(\xi)$ behaves as $1/\xi^2$ for large values of ξ. Thus for small values of k_z real part of $K_{||}$ is given by

$$\mathrm{Re}(K_{||}) \simeq 1 - \frac{\omega_p^2}{\omega^2}$$

which is less than zero for $\omega < \omega_p$, hence $\tan^{-1}(\mathrm{Im}K_{||}/\mathrm{Re}K_{||}) \simeq \pi$. Therefore first term in 7.7 vanishes and only the second term contributes to $R_{||}$. Then the input resistance for a triangular current distribution on the antenna is again given by 7.10 with $F(k_o\ell)$ as following

$$F(k_o\ell) = \left(\frac{c}{V_o}\right)^3 (k_o\ell)^2 \frac{1}{\pi} \int_{V_o/c}^{\infty} dx(x^2 - V_o^2/c^2)\left(\frac{\sin\left(\frac{x\omega\ell}{2V_o}\right)}{\frac{x\omega\ell}{2V_o}}\right)^4 \tan^{-1}\left(\frac{\mathrm{Im}K_{||}}{\mathrm{Re}K_{||}}\right) \tag{7.14}$$

$F(k_o\ell)$ in 7.14 is evaluated numerically and its behavior as a function of the dipole length ℓ is given in Figure 7.1.

When the length of the dipole is such that $\ell >> \lambda_d$, the two models of the plasma give almost same values for R. But for $\ell << \lambda_d$ kinetic model gives larger values of R than the fluid model. For very small values of $\ell << \lambda_d$, the antenna is very effective in radiating the short wavelength waves which are very susceptible to the Landau damping. Thus the energy is transferred from the fields to the electrons. The electrons are heated up. This account for the larger value of $R_{||}$ in kinetic model than the fluid model. For $\ell >> \lambda_d$

the antenna excites waves of longer wavelength which are not as much susceptible to the Landau damping and therefore the two models give comparable values of R .

For very small lengths $\ell << \lambda d$ the integral in 7.14 is logrithmically divergent. For such lengths $[\sin(x\omega\ell/2V_o)/(x\omega\ell/2V_s] \simeq 1$. For large values of k_z it can be seen from 7.13 that $Im(K_{||}) \propto k_z^{-3}$ and $Re(K_{||})$ can be shown to be unity. Therefore $\tan^{-1}(ImK_{||}/ReK_{||})$ behaves as k_z^{-3}. Thus the integrand in 7.14 falls off as x^{-1} giving the logarithmic divergence. However if we truncate the integral at $x = V_o/\omega\ell$, $R_{||}$ will behave as $\ell^2 \log(1/\ell)$. In the limit ℓ tends to zero $R_{||}$ also goes to zero.

7.3 Case $\omega > \omega_p$

For this case in the cold plasma approximation Seshadri [17] has shown that the radiation resistance of a short electric dipole antenna is the same as in the free space. The inclusion of the electron temperature in the theory gives an additional term in the radiation resistance. We describe this additional contribution as the radiation into a hot plasma mode. This additional term is found to be much greater than the usual electromagnetic mode radiation term for lengths of the dipole antenna of the order of Debye length. When the length is of the order of the free space wavelength the antenna radiates primarily in to the electromagnetic mode.

For the fluid model of the plasma $\tan^{-1}(ImK_{||}/ReK_{||}) = 0$ for $0 < k_z < k_o$. $\tan^{-1}(ImK_{||}/ReK_{||})$ is non-zero only when $\omega/V_s\sqrt{1 - \omega_p^2/\omega^2} < k_z < \omega/V_s$. Thus we obtain from 7.7 and 7.9

$$R = \frac{1}{4\pi}\sqrt{\frac{\mu_o}{\varepsilon_o}}\; F(k_o\ell) \qquad (7.15)$$

where $$F(k_o\ell) = (k_o\ell)^2 \int_o^1 (1-x^2)\left\{\frac{\sin(\frac{k_o x\ell}{2})}{\frac{k_o x\ell}{2}}\right\}^4 dx$$

$$+ \left(\frac{c}{V_s}\right)^3 (k_o\ell)^2 \int_{\sqrt{1-\omega_p^2/\omega^2}}^1 (x^2 - V_s^2/c^2)\left\{\frac{\sin(\frac{\omega}{V_s}\frac{x\ell}{2})}{\left(\frac{\omega x\ell}{2V_s}\right)}\right\}^4 dx \qquad (7.16a)$$

From the foregoing we see that there are two terms contributing to the total input resistance, since the plasma is lossless, the input resistance will be equal to the radiation resistance. If we recall the discussion in section (5.2) for the case $\omega > \omega_p$ we immediately realize that the first term in 7.16a corresponds to the radiation into the <u>electromagnetic mode</u>, while the second term corresponds to the hot <u>plasma mode of radiation</u>. The second term is a hot plasma effect. The cold plasma approximation does not give this term.

The Figure 7.2 shows the dependence of the input resistance on the antenna length. When $\ell << \lambda_d$ the input resistance varies as ℓ^2. When $\lambda_d << \ell << \lambda_o$ (the free space wavelength) input resistance falls faster than ℓ^{-1}, but again when $k_o\ell \geq 1$ it increases as ℓ^2.

Considering <u>kinetic theory model</u> of the plasma, $\tan^{-1}(\mathrm{Im}K_{||}/\mathrm{Re}K_{||})=0$ when $|k_z| < k_o$, hence we have

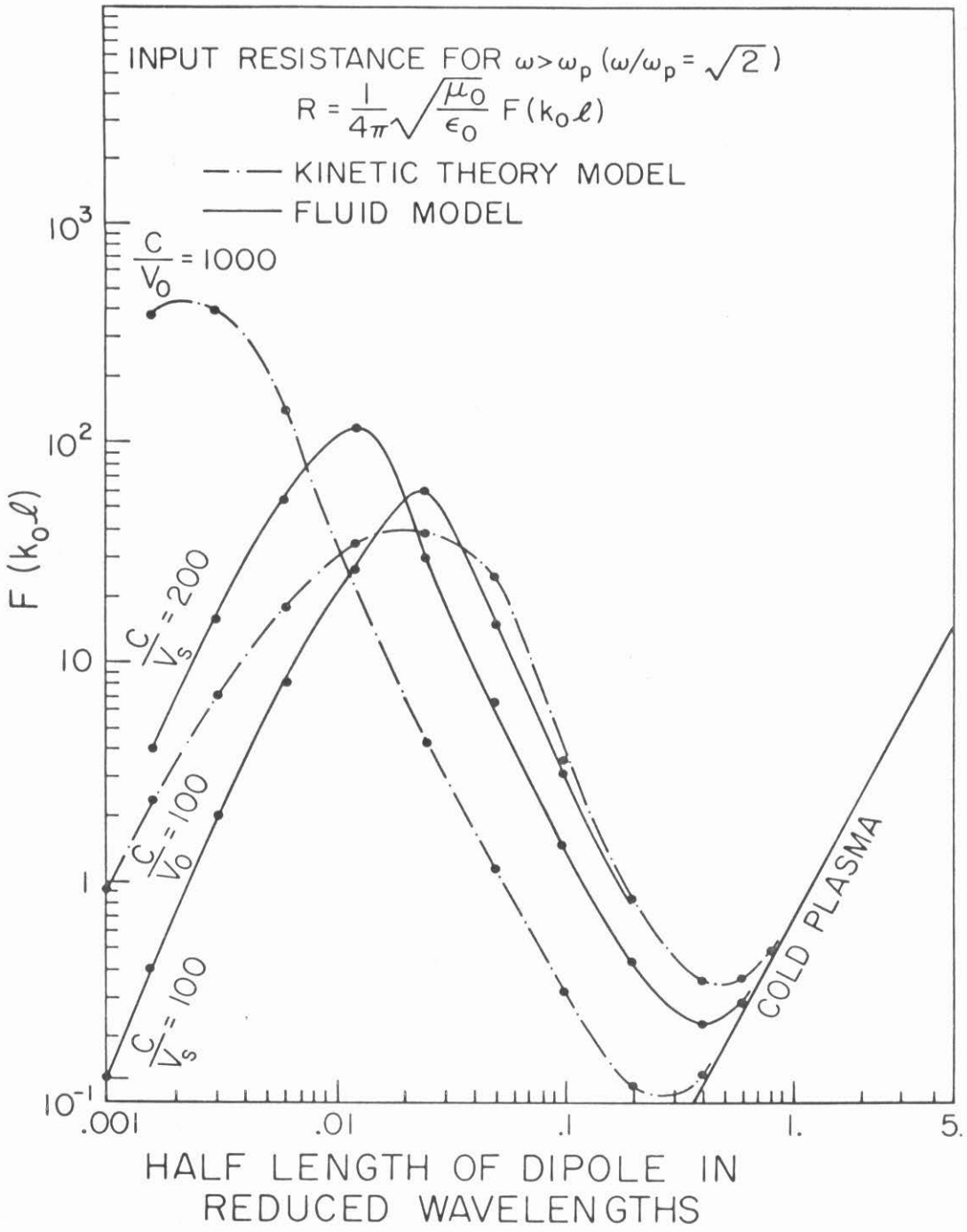

Figure 7.2 Functional dependence of the input resistance on dipole length for $\omega > \omega_p$

$$F(k_o\ell) = (k_o\ell)^2 \int_o^1 (1 - x^2) \left(\frac{\sin(\frac{xk_o\ell}{2})}{\frac{xk_o\ell}{2}} \right)^4 dx$$

$$+ \left(\frac{c}{V_o}\right)^3 (k_o\ell)^2 \int_{V_o/c}^{\infty} (x^2 - \frac{V_o^2}{c^2}) \left\{ \frac{\sin(\frac{\omega}{V_o} \frac{x\ell}{2})}{\frac{\omega x\ell}{2V_o}} \right\}^4 \frac{1}{\pi} \tan^{-1}\left(\frac{ImK_{II}}{ReK_{I}}\right) \qquad (7.16b)$$

Again in this case the integral in the second term diverges logarithmically as the length of the dipole approaches zero, and this term behaves as $\ell^2 \log(1/\ell)$. Figure 7.2 displays the input resistance as a function of the length of the dipole for this model of the plasma. For lengths much less than the Debye length the kinetic model gives a larger value of R_{11} than the fluid model. But when the length is comparable to the free space wavelength both the models give same input resistance. For these lengths the antenna is primarily a radiator of the electromagnetic waves on which Landau damping has almost no effect. Thus the two models give comparable results.

7.4 The Radiated Power

So far in this chapter we were concerned with the input power and the resistance. In Chapter IV it was shown that in a lossless fluid model of the plasma the input and the radiated power are equal. For the kinetic theory model, the plasma medium is lossy because of the Landau damping. In this section we investigate how the power radiated depends upon the distance from the antenna and it compares with the input power for the kinetic theory model of the plasma. The

power radiated P_r across a cylindrical surface of radius ρ is given by equation 4.8 and it is rewritten

$$P_r = \frac{\omega\mu_o}{16}\rho\ \mathrm{Im}\int_o^\infty dk_z\left(1-\frac{k_z^2}{k_o^2}\right)\hat{J}_s^2(k_z)\ \xi^* H_o^{(2)}(\xi\rho)H_1^{(2)}(\xi\rho) \qquad (7.17)$$

Here $n = 2$ has been taken and sign of the square root in the expression of ξ is chosen in such a way that $\mathrm{Im}(\xi) < 0$.

Substituting for $J_s(k_z)$ the expression in 7.9 we obtain

$$P_r = \frac{1}{8\pi}\sqrt{\frac{\mu_o}{\varepsilon_o}}\,G(\rho,\ell) \qquad (7.18)$$

where $$G(\rho,\ell) = \frac{\pi}{2}\rho\ (k_o\ell)^2\mathrm{Im}\int_o^\infty dk_z\left[1-\frac{k_z^2}{k_o^2}\right]\left[\frac{\sin(\frac{k_z\ell}{2})}{k_z\ell/2}\right]^4 \xi^* H_o^{(2)}(\xi\rho)H_1^{(2)}(\xi\rho) \qquad (7.19)$$

For small values of ρ the integral in 7.19 can be evaluated numerically. When ρ is large, it is hard to calculate the hankel functions accurately by numerical methods. But then the Hankel functions can be replaced by their asymptotic expansions. The large argument approximations are adequate because $\xi = 0$ only when $k_z = k_o$ and there the integrand is zero and integration does not contribute significantly to the integral. It follows that,

$$G(\rho,\ell) = (k_o\ell)^2\mathrm{Re}\int_o^\infty dk_z\left(\frac{k_z^2}{k_o^2}-1\right)\left(\frac{\sin(\frac{k_z\ell}{2})}{\frac{k_z\ell}{2}}\right)^4 \frac{\xi^*}{|\xi|}\,e^{2\rho\,\mathrm{Im}(\xi)} \qquad (7.20)$$

$\omega<\omega_p$

It was shown in section (7.2.2) that for $k_z < k_o$

$\mathrm{Im}(K_{\|}) \simeq 0$ and $\mathrm{Re}(K_{\|}) \simeq 1 - \omega_p^2/\omega^2$. Since $\xi = \sqrt{(k_o^2-k_z^2)K_{\|}}$, ξ is

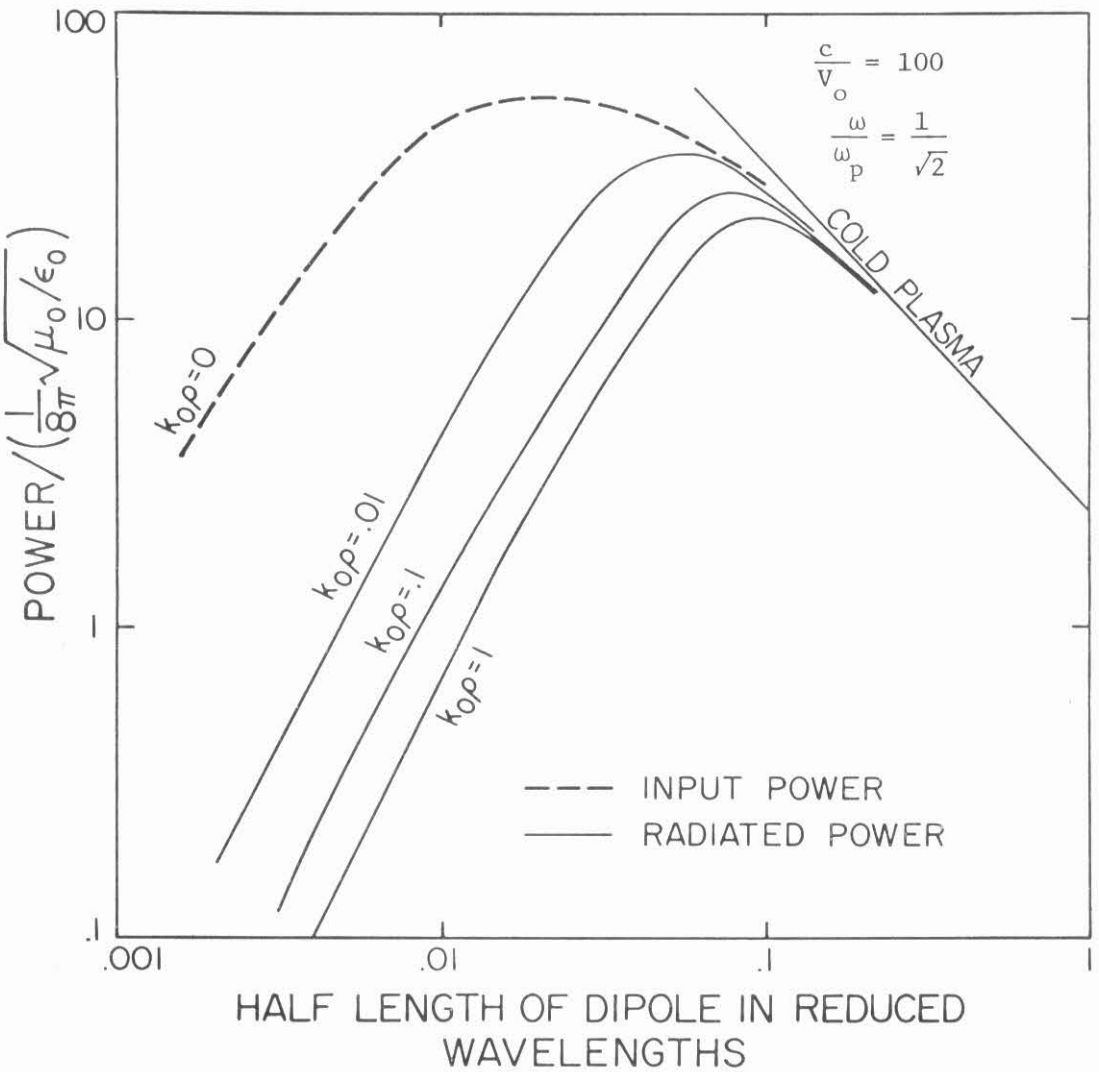

Figure 7.3 Functional dependence of the radiated power on dipole length for $\omega < \omega_p$.

almost imaginary. Therefore the contribution to $G(\rho,\ell)$ from values of k_z in the range $0 < k_z < k_o$ is negligible. For $k_z > k_o$ over a certain range of values of k_z $\mathrm{Im}(\xi)$ is very small but it is non-zero. Thus this will cause slow exponential damping of the power. Figure 7.3 displays power radiated against length of the dipole for $k_o\rho = .01,.1,1.$ These curves are obtained by numerical evaluation of the integral in eqn. 7.19. Also, the input power is given here. We can see from this figure that for length of the dipole $\ell << \lambda_d$ the radiated power is strongly damped, while for $\ell >> \lambda_d$ the damping is very weak. The reason for this is that for $\ell << \lambda_d$ the dipole excites the slow waves, which are strongly susceptible to the Landau damping. When $\ell >> \lambda_d$ the fast waves are excited and these are not much affected by the damping. Also, for very short lengths $(\ell << \lambda_d)$ the power behaves as ℓ^2 when $\rho \neq 0$. Thus the $\ell^2\log(1/\ell)$ behavior of the input power does not appear in the radiated power far from the antenna.

$\underline{\omega < \omega_p}$

When $\omega > \omega_p$ ξ is almost pure real for $0 < k_z < k_o$, and for $k_z > k_o$, $\mathrm{Im}(\xi)$ is quite large. Thus for large ρ the radiation into the hot plasma mode is damped away, and the power is radiated mostly in the electromagnetic mode. The radiated power behaves as ℓ^2.

VIII. DIPOLE ORIENTED PERPENDICULAR TO $\underline{B}_o$

In a magnetoplasma the input resistance of a dipole antenna will depend upon its orientation with respect to the biasing d.c. magnetic field $\underline{B}_o$. We have explored in detail the case of the dipole parallel to $\underline{B}_o$. The case of the dipole perpendicular to $\underline{B}_o$ can also be solved. In this case the flow of the source current in the perpendicular direction and of the plasma current in the parallel direction makes this problem very cumbersome. In this chapter we outline the method of solution and present some interesting features of this problem, although we do not obtain detailed results.

We assume that the dipole antenna is oriented along the x-axis while the magnetostatic field ($\underline{B}_o=\infty$) is along the z-axis. Rewriting equation (2.6) we have

$$\nabla^2\underline{E} + \omega^2\mu_o\varepsilon_o\underline{E} = -i\omega\mu_o\underline{J} - \frac{i}{\omega\varepsilon_o}\nabla\nabla\cdot\underline{J} \tag{8.1}$$

where $$\underline{J} = J_s\,\underline{e}_x + J_p\,\underline{e}_z$$

The foregoing equations can be written in component form to give

$$[\nabla^2 + k_o^2]\,E_x = -i\omega\mu_o J_s - \frac{i}{\omega\varepsilon_o}\frac{\partial^2}{\partial x^2}J_s - \frac{i}{\omega\varepsilon_o}\frac{\partial}{\partial x}\frac{\partial}{\partial z}J_p \tag{8.2}$$

$$[\nabla^2 + k_o^2]\,E_y = -\frac{i}{\omega\varepsilon_o}\frac{\partial}{\partial y}\frac{\partial}{\partial x}J_s - \frac{i}{\omega\varepsilon_o}\frac{\partial}{\partial y}\frac{\partial}{\partial z}J_p \tag{8.3}$$

$$[\nabla^2 + k_o^2]\,E_z = -i\omega\mu_o J_p - \frac{i}{\omega\varepsilon_o}\frac{\partial}{\partial z}\frac{\partial}{\partial x}J_s - \frac{i}{\omega\varepsilon_o}\frac{\partial^2}{\partial z^2}J_p \tag{8.4}$$

Carrying out the Fourier transform of equations 8.2, 8.3 and 8.4 and substituting the expression for J_p given in equation 2.10 we obtain

$$\hat{E}_x(\underline{k}) = -i\omega\varepsilon_o \frac{\left(1-\frac{k_x^2}{k_o^2}\right)\hat{J}_s(\underline{k})}{k_o^2 - k^2} + \frac{i}{\omega\varepsilon_o} \frac{k_x^2 k_z^2 (K_{||}-1)\hat{J}_s(\underline{k})}{[K_{||}(k_o^2-k_z^2)-k_x^2-k_y^2]\ [k_o^2-k^2]} \quad (8.5)$$

$$\hat{E}_y(\underline{k}) = \frac{i}{\omega\varepsilon_o} \frac{k_y k_x \hat{J}_s(\underline{k})}{k_o^2-k^2} + \frac{i}{\omega\varepsilon_o} \frac{k_y^2 k_z^2 (K_{||}-1)\hat{J}_s(\underline{k})}{[K_{||}(k_o^2-k_z^2)-k_x^2-k_y^2]\ [k_o^2-k^2]} \quad (8.6)$$

$$\hat{E}_z(\underline{k}) = \frac{i}{\omega\varepsilon_o} \frac{k_z k_x \hat{J}_s(\underline{k})}{K_{||}(k_o^2-k_z^2)-(k_x^2+k_y^2)} \quad (8.7)$$

where a function $\hat{G}(\underline{k})$ is the Fourier transform of $G(\underline{r})$ given by

$$\hat{G}(\underline{k}) = \int_{-\infty}^{\infty} G(\underline{r})\ e^{i\underline{k}\cdot\underline{r}}\, d\underline{r} \quad (8.8)$$

and $$\underline{k} = k_x\, \underline{e}_x + k_y\, \underline{e}_y + k_z\, \underline{e}_z$$

The above expressions for the transform of the electric field components are for a general current distribution, but the dipole current is restricted to flow only in the x-direction. Now the input resistance $R_\perp$ is as before given by

$$R_\perp = -\mathrm{Re} \int_V \underline{E}(\underline{r})\cdot\underline{J}^*(\underline{r})\ dV \quad (8.9)$$

where V is the volume occupied by the source current. Using Parseval theorem the above expression for $R_\perp$ can be written in terms of $E_x(\underline{k})$ and $J(\underline{k})$. Then the use of equation 8.5 gives

$$R_{\perp} = + \frac{\omega\mu_o}{8\pi^3} \text{ Im} \int \frac{1-\frac{k_x^2}{k_o}}{k^2-k_o^2} \hat{J}_s^2(\underline{k}) \, d^3\underline{k}$$

$$+ \frac{1}{8\omega\varepsilon_o\pi^3} \text{ Im} \int \frac{k_x^2 k_z^2 (K_{||}-1)\hat{J}_s^2(\underline{k})}{(k^2-k_o^2)[k_x^2+k_y^2-K_{||}(k_o^2-k_z^2)]} d^3\underline{k} \qquad (8.10)$$

when $K_{||} = 1$ the second term in the above expression is zero and (8.10) reduces to the radiation resistance of a short dipole antenna in the free space. The equation (8.10) gives the input resistance for an x-directed dipole with a general current distribution. In this form it is difficult to evaluate the integral. For a short dipole for which $J_s(\underline{k}) \simeq \ell$ (length of the dipole) the integral in (8.10) can be simplified. With this assumption the first integral in (8.10) can be easily evaluated and, denoting it by R_1, we have

$$R_1 = - \frac{\omega\mu_o}{4\pi^2} \ell^2 \text{Im} \int_0^{\infty} dx \, (1 - \frac{x^2}{k_o^2}) \ell n \, (x^2-k_o^2) \qquad (8.11)$$

We denote the second term by R_2. Letting $k_x = k\cos\theta$, $k_y = k\sin\theta$ and performing integration with respect to θ and k we obtain

$$R_2 = \frac{R^2}{8\omega\varepsilon_o\pi^2} \text{ Im} \int_0^{\infty} k_z^2 [K_{||} - K \ell n \, K - (K_{||}-1) \ln(k_z^2-k_o^2)] dk_z \qquad (8.12)$$

Combining R_1 and R_2 and replacing k_z by x we obtain

$$R_{\perp} = - \frac{\omega\mu_o}{4\pi^2} \ell^2 \text{ Im} \int_0^{\infty} dx \, \ell n(x^2-k_o^2) \left[1 - \frac{3x^2}{2k_o^2} + \frac{1}{2} K_{||} \frac{x^2}{k_o^2}\right]$$

$$+ \frac{\ell^2}{8\omega\varepsilon_o\pi^2} \text{ Im} \int_0^{\infty} x^2 \, K_{||} (1-\ell n K_{||}) dx \qquad (8.13)$$

where $K_{||}(k_z)$ is taken to be $K_{||}(x)$. The signs of $\ln(x^2-k_o^2)$ and $\ln(K_{||})$ should be chosen in such a way that $R_{\perp}$ given by (8.13) is always positive.

Cold Plasma

In the cold plasma approximation $K_{||}=1-\frac{\omega_p^2}{\omega^2}$, which is real. For $\omega<\omega_p$ $K_{||}$ becomes negative. Then the integral in the second term of 8.13 diverges. This divergence in the input resistance can be removed by assuming a current distribution where Fourier transform falls off rapid enough with the wave number k_z.

For $\omega>\omega_p$ we obtain from 8.13

$$R_{\perp} = \frac{1}{24\pi}\sqrt{\frac{\mu_o}{\varepsilon_o}}\,(k_o\ell)^2\,\left[3 + (1-\frac{\omega_p^2}{\omega^2})\right] \qquad (8.14)$$

Kuehl [3] derived the above expression by Poynting vector method. Also, he pointed out the divergence in the input resistance for $\omega<\omega_p$. It should be noted from 8.14 that when the dipole is oriented perpendicular to B_o, the input resistance depends upon the plasma frequency. For a dipole oriented along B_o the input resistance in a cold plasma is given by equation (7.19) with $F(k_o\ell)$ as the first term in (7.20). For short lengths it can be written as

$$R_{||} = \frac{1}{6\pi}\sqrt{\frac{\mu_o}{\varepsilon_o}}\,(k_o\ell)^2$$

It can be seen that $R_{||}$ is independent of ω_p. For any arbitrary orientation of the dipole the input resistance will in general be function of the plasma density.

Hot Plasma

In case of the dipole parallel to B_o only the argument of $K_{||}$ appeared in the expressions for the input resistance. But in the perpendicular case the magnitude of $K_{||}$ appears in the expressions for R. Since $K_{||}$ in fluid model is singular when $k_z = \frac{\omega}{v_o}$, it fails to give realistic result in this case. Therefore, the kinetic description of the plasma should be used. For this model of the plasma $Im(K_{||}) \sim x^{-3}$ $(x=k_z)$ and $Re(K_{||}) \simeq 1$ for large values of x. Therefore $\ell n(K_{||}) \propto \tan^{-1} \frac{ImK_{||}}{ReK_{||}}$ behaves as x^{-3}. Thus the integrand in the second term of (8.13) falls as $\frac{1}{x}$ and the integral diverges logarithmically. Therefore we conclude here that the infinitesimal dipole does not present a physical problem. In order to obtain physically reasonable results an antenna of finite size must be considered.

IX. CONCLUSIONS AND DISCUSSIONS

In this paper the input and the radiation resistances, and the field of a short electric dipole antenna embedded in a hot uniaxial plasma have been studied.

The addition of electron thermal velocities to the theory modifies the cold plasma results substantially. In a cold uniaxial plasma when $\omega < \omega_p$ the radiation resistance of a dipole antenna of length ℓ varies as ℓ^{-1}, and thus it approaches infinity as the length approaches zero. In the fluid model of a hot plasma the radiation resistance remains always finite. If the length of the dipole $\ell << \lambda_d$ (Debye length), radiation resistance varies as ℓ^2. Only when $\ell >> \lambda_d$ does the radiation resistance vary as ℓ^{-1}.

In the cold plasma approximation the radiation resistance $R_o = \frac{1}{6\pi} \sqrt{\mu_o/\varepsilon_o}\, (k_o \ell)^2$ for $\omega > \omega_p$. This also gives the radiation resistance of a short dipole antenna in free space. For the fluid model of a hot plasma an additional term appears in the expression for the radiation resistance. This term is due to radiation into a hot plasma mode and can be much larger than R_o when the dipole length is smaller than, or of the order of, λ_d. But when the length becomes of the order of the free space wavelength, this term becomes negligible compared to R_o.

When we include Landau damping by using a kinetic description of the plasma, we have to distinguish between the input power and the radiated power. The radiated power depends upon the distance from the

antenna. In this situation we can define a unique input resistance for the dipole antenna, but a unique radiation resistance cannot be defined.

It is found that the input resistance behaves as $\ell^2 \log(1/\ell)$. This logarithmic behavior does not appear in the radiated power far from the antenna. The logarithmic behavior of the input resistance can be removed by considering a dipole of finite thickness.

For $\omega < \omega_p$ when $\ell >> \lambda_d$ the radiated power is Landau damped very weakly. But for $\ell << \lambda_d$ the damping is strong. For $\omega > \omega_p$ the power radiated into the hot plasma mode is quickly damped, and far from the source the power is contained mainly in the electromagnetic mode.

For $\omega < \omega_p$ the hot plasma effects give finite field on the conical surface of semicone angle $\sin^{-1}(\omega/\omega_p)$, where the fields are singular for a cold plasma. In this case the dipole excites two waves, a slow wave and a fast wave inside the cone. The net field will be the result of the interference of these waves. The slow wave is a hot plasma effect. When $\omega > \omega_p$ in addition to the electromagnetic mode the antenna excites a hot plasma mode. The hot plasma mode is confined in a conical region centered along $\underline{B}_o$. The slow wave for $\omega < \omega_p$ and the hot plasma mode for $\omega > \omega_p$ are very susceptible to collisional and Landau damping.

Near the antenna even in the presence of damping processes, interference among the propagating waves is noted. The interference phenomenon and the occurrence of cones in the field patterns for $\omega < \omega_p$ can be useful from the viewpoint of diagnostics in small volume

laboratory magnetoplasma. This technique has been demonstrated by Fisher and Gould [20,21].

For a dipole whose orientation is not parallel to the magnetic field $\underline{B}_o$, the fluid model fails to give realistic results, while the kinetic description of the plasma can predict physically reasonable and useful results. It is believed that the fluid model fails here because of our assumption that $B_o = \infty$. In this assumption the thermal motion of the electrons perpendicular to the magnetic field are neglected. By including the perpendicular thermal motion in the theory, the fluid model may be made useful for predicting the antenna properties for any arbitrary orientation. Therefore there is a definite need for a hot plasma theory valid for finite magnetic field B_o.

In an anisotropic plasma the phase and group velocities are, in general, not parallel. This has caused some confusion regarding the allowed directions of propagation. The transmission of signals and information is determined by the group velocity. In some directions with respect to $\underline{B}_o$ where plane wave phase propagation is not possible, it is possible for signals to propagate. For example, when $\omega_p = \frac{\sqrt{3}}{2}\omega$, in a uniaxial plasma, the plane wave phase propagation is allowed only in a cone of semicone angle 30°, but the signals can propagate beyond this angle up to 60°. It should be emphasized that when determining whether propagation of signals between two points in an anisotropic plasma is possible, one should examine the allowed direction of group velocity and the group velocity plots [16], rather than allowed directions of phase velocity and customary phase velocity plots [23].

In light of the agreement between some of the theoretical calculations in this paper and available experimental results [19], it is encouraging to note that even such an idealized model of the problem can describe its physics at least in a qualitative way. For quantitative agreement between experiment and theory, the sheath around the antenna, the determination of the correct current distribution on the antenna, and the valid boundary conditions between the antenna and the plasma, etc. must be taken into account.

There have been very few experimental investigations of sources in anisotropic plasma. There is a definite need for measurements of antenna impedances. This measurement can verify the functional dependence of the input resistance on the antenna dimension.

REFERENCES

1. Bunkin, F. V. "On Radiation in Anisotropic Media", Soviet Physics JETP 5, 277-283 (1957).

2. Kogelnik, H., "On Electromagnetic Radiation in Magneto-ionic Media", J. Research, NBS 64D, Sept.-Oct., 1960. Also, "The Radiation Resistance of an Elementary Dipole in Anisotropic Plasmas", Fourth International Conference on Ionization Phenomena in Gases, North-Holland Publ. Co., Amsterdam, Netherlands, 1960.

3. Kuehl, H. H., "Electromagentic Radiation from an Electric Dipole in a Cold Anistropic Plasma", Phys. Fluids 5, 1095-1103 (1962). Also, "Radiation from an Electricl Dipole in an Anisotropic Cold Plasma", Antenna Laboratory Report No. 24, California Institute of Technology, Pasadena, California (1960).

4. Staras, H., "The Impedance of an Electric Dipole in a Magneto-ionic Medium", IEEE Trans. AP-12, 695 (1964). Also, "The Infinity Catastrophe Associated with Radiation in Magneto-ionic Media", Radio Science 1 (new series), September 1960, p. 1013.

5. Seshadri, S. R., "Radiation Resistance of Elementary Electric-Current Sources in a Magneto-ionic Medium", Proc. IEE 112, 1856 (1965).

6. Lee, K. S. H., and Papas, C. H., "Irreversible Power and Radiation Resistances of Antenna in Anisotropic Ionized Gases", J. Research NBS/USNC-URSI 69D, 1313 (1965).

7. Kuehl, H. H., "Resistance of a Short Antenna in a Warm Plasma", Radio Science 1 (new series), 218 (1966).

8. Wait, James R., "Radiation from Sources Immersed in Compressible Plasma Media", Canadian J. Phys. 42, 1760 (1964).

9. Deschamps, G. A. and Kesler, A. B., "Radiation on an Antenna in a Compressible Magnetoplasma", Radio Science 2 (new series), 757 (1967).

10. Chen, H. C., "Radiation Characteristics of an Electric Dipole in a Warm, Anisotropic Plasma", J. Appl. Phys. 40, 4068 (1969).

11. Tunaley, J. K. E., and Grard, R. J. L., "The Impedance of Probe in a Warm Plasma", Ann. Geophys. 25, 55 (1969).

12. Fisher, R. K., "Resonance Cones in the Field Pattern of a Short Radio Frequency Probe in a Warm Anisotropic Plasma", Ph.D. Thesis, California Institute of Technology, April 1970.

13. Fried, B. D., and Conte, S. D., The Plasma Dispersion Function, Academic Press, New York, 1961.

14. Papas, C. H., Theory of Electromagnetic Wave Propagation, McGraw-Hill Book Company, 1965; p. 16.

15. Holt, E.H., and Haskel, R.E, Plasma Dynamics, MacMillan Co., New York, 1965, pp. 412-419.

16. Gould, R. W., and Fisher, R. K., "Phase and Group Velocity in an Anisotropic Plasma", Proc. 9th Int. Conference on Ionization Phenomena in Gases, Bucharest, Ramania, 1969.

17. Seshadri, S. R., "Radiation Resistance of a Linear Current Filament in a Simple Anisotropic Medium", IEEE Trans. on Antennas and Propagation, Sept. 1965, p. 819.

18. Erdelyi, A., Asymptotic Expansions, Dover Publications, Inc., New York, 1956, p. 51.

19. Plesset, M. S. and Wu, T. Y., "Water Waves Generated by Thin Ships", Jour. Ship Research, November 1960, pp. 25-36.

20. Fisher, R. K., and Gould, R. W., "Resonance Cone Structure in Warm Anisotropic Plasma", Phys. Letters 31A, 256 (1970).

21. Fisher R. K., and Gould, R. W., "Resonance Cones in the Field Pattern of a Short Antenna in an Anisotropic Plasma", Phys. Rev. Letters 22, pp. 1093-1095 (1969).

22. Balmain, K. G., "The Impedance of a Short Dipole Antenna in a Magnetoplasma", IEEE Trans. AP-12, 605 (1964).

23. Allis, W. P., Buchsbaum, S. J., and Bers, A., Waves in Anisotropic Plasma, M.I.T. Press, Cambridge, Mass. (1963), Chapter 3.